CENTRAL RESEARCH LIBRARY
DOCUMENT COLLECTION

MARTIN MARIETTA ENERGY SYSTEMS LIBRARIES
3 4456 0286819 0

ORNL-3103
UC-25 – Metals, Ceramics, and Materials

DIMENSIONAL BEHAVIOR OF THE EXPERIMENTAL GAS-COOLED REACTOR FUEL ELEMENT AT ELEVATED TEMPERATURES

W. R. Martin
J. R. Weir

CENTRAL RESEARCH LIBRARY
DOCUMENT COLLECTION
LIBRARY LOAN COPY
DO NOT TRANSFER TO ANOTHER PERSON
If you wish someone else to see this document, send in name with document and the library will arrange a loan.

OAK RIDGE NATIONAL LABORATORY
operated by
UNION CARBIDE CORPORATION
for the
U.S. ATOMIC ENERGY COMMISSION

LEGAL NOTICE

This report was prepared as an account of Government sponsored work. Neither the United States, nor the Commission, nor any person acting on behalf of the Commission:

A. Makes any warranty or representation, expressed or implied, with respect to the accuracy, completeness, or usefulness of the information contained in this report, or that the use of any information, apparatus, method, or process disclosed in this report may not infringe privately owned rights; or

B. Assumes any liabilities with respect to the use of, or for damages resulting from the use of any information, apparatus, method, or process disclosed in this report.

As used in the above, "person acting on behalf of the Commission" includes any employee or contractor of the Commission, or employee of such contractor, to the extent that such employee or contractor of the Commission, or employee of such contractor prepares, disseminates, or provides access to, any information pursuant to his employment or contract with the Commission, or his employment with such contractor.

ORNL-3103

Metals, Ceramics, and Materials
TID-4500 (16th ed.)

Contract No. W-7405-eng-26

METALLURGY DIVISION

DIMENSIONAL BEHAVIOR OF THE EXPERIMENTAL GAS-COOLED REACTOR FUEL ELEMENT AT ELEVATED TEMPERATURES

W. R. Martin and J. R. Weir

DATE ISSUED

JUL 19 1961

OAK RIDGE NATIONAL LABORATORY
Oak Ridge, Tennessee
operated by
UNION CARBIDE CORPORATION
for the
U. S. ATOMIC ENERGY COMMISSION

MARTIN MARIETTA ENERGY SYSTEMS LIBRARIES

3 4456 0286819 0

DIMENSIONAL BEHAVIOR OF THE EXPERIMENTAL GAS-COOLED REACTOR FUEL ELEMENT AT ELEVATED TEMPERATURES

W. R. Martin and J. R. Weir

ABSTRACT

The Experimental Gas-Cooled Reactor (EGCR) fuel assemblies consist of a cluster of seven fuel elements contained in a graphite sleeve. Each element is composed of hollow cylindrical UO_2 pellets encapsulated in a type 304 stainless steel tube. The difference in the mechanical properties of the cladding and the fuel pellets and the existence of the annular pellets create uncertainties in predicting the behavior of the fuel element at elevated temperatures.

The dimensional behavior of the fuel element was determined in an apparatus which simulated the thermal conditions predicted for the EGCR. Particular emphasis was placed on determining the relationship between the fuel temperature and axial expansion, the radial expansion characteristics of the fuel, the effect of cladding and fuel interaction on heating and subsequent cooling, the effect of rapid temperature excursions on the degradation of the fuel, and accumulative effects in the fuel element due to thermal cycling.

The program was separated into two parts. First, the dimensional behavior of the EGCR fuel element was determined when a radial gap existed between the cladding and the fuel pellet, and secondly, the behavior of the fuel element was observed after the cladding had been collapsed onto the pellet by means of external pressure.

An element that contains a radial gap between the cladding and the fuel pellet was found to respond to thermal cycling in the same manner that the individual components would react if subjected to the same thermal conditions and tested separately. Both the axial and radial expansion of the fuel pellet are very nearly a function of the maximum central temperature. The axial expansion of the fuel pellet column can be reduced appreciably at elevated temperatures by "dishing" the ends of the pellets. The pellets fracture radially and circumferentially upon heating, but redistribution of the fuel does not occur.

If no radial gap exists between the fuel and the cladding, the expansion characteristics of the element during thermal cycling are a function of the fuel temperature, cladding temperature, and the external pressure exerted on the element by the coolant stream. Thermal cycling may introduce plastic axial strains into the cladding depending upon the details of the temperature cycle and the pressure conditions.

INTRODUCTION

The EGCR is a combined experimental and power demonstration reactor to be constructed at Oak Ridge, Tennessee. It is a helium-cooled graphite-moderated reactor fueled with enriched uranium dioxide. The fuel assembly consists of a cluster of seven fuel elements contained in a cylindrical graphite sleeve. Each element is composed of high-density hollow UO_2 pellets encapsulated in a type 304 stainless steel tube. The fuel assembly is shown in Fig. 1.

While the use of oxide fuels has been quite broad, many of the properties of these fuels are poorly understood so that application under a new set of reactor conditions results in a degree of uncertainty as to its behavior. This inability to predict the detailed behavior of oxide fuel generally leads to an in-pile testing program for each new application. However, the peculiarity of irradiation testing is such that application of experimental data to different sets of conditions to predict quantitative results is difficult. Therefore, current fuel element design depends upon the understanding, at least in a semi-quantitative sense, of how the material can be expected to behave.

Basically the EGCR fuel body, compared to a solid pellet, has the advantage that it provides a space which can accommodate the fission gas released from the oxide. Further, the hollow pellet eliminates fuel from the high-temperature region where redistribution by sublimation or melting is expected in the solid pellet. The performance of this pellet has been predicted largely on the basis of experiments with solid pellets in which a central core developed during irradiation. Irradiation experiments with smaller cored pellets provide the

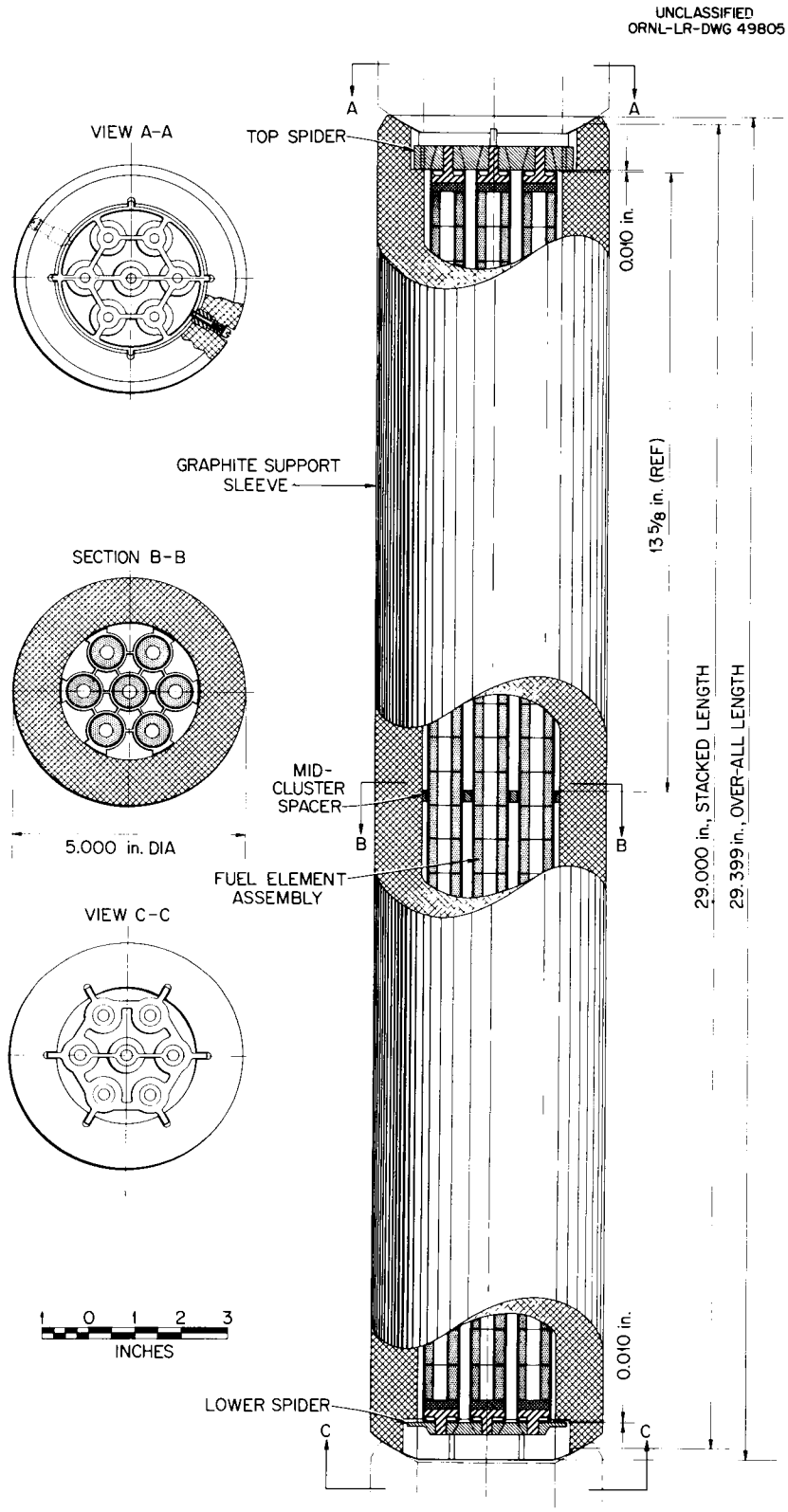

Fig. 1. View of EGCR Fuel Assembly.

principal direct experience with this shape.[1,2] Both of the above experiments have shown that the geometry is quite stable inasmuch as gross longitudinal displacement of the fuel has not been observed. The most likely explanation of this stability is that the cracks that develop in the UO_2 are generally radial and few in number so that the pieces bridge or key themselves in their original positions. In addition, it has been proposed that small cracks which may develop near the inner UO_2 surface tend to heal themselves due to sintering in the high-temperature areas. Thus, the observations are consistent in showing that gross migration of fuel toward the bottom of the vertical fuel element should not occur in a fuel assembly consisting of small-diameter annular pellets.

The clearance between the outside surface of the UO_2 and the inside surface of the tubing is that required for ease of assembly or that determined from detailed consideration of the behavior of the tubing when subjected to external pressure at operating temperatures.

The behavior of the radial gap during irradiation is an important consideration in predicting the behavior of the fuel element. In several experiments evaluated to date, postirradiation inspection has shown that the initial gap present at assembly has disappeared during irradiation.[3-5] This has been true for a great variety of exposure conditions and is the behavior to be expected in irradiated bulk UO_2 bodies. Several mechanisms, including radial cracking and mechanical readjustment of the fuel, volatilization of part of the high-temperature UO_2 with redeposition to the outside of the fuel body, and sintering of the UO_2 resulting in the migration of fuel away from the hotter central regions

---

[1] J. A. L. Robertson and A. S. Bain, UO_2 Irradiation of Short Duration, CRFD-825 (April, 1959).

[2] W. K. Barney and B. D. Wemple, Metallography of Irradiated UO_2 Containing Fuel Elements, KAPL-1836 (January, 1958).

[3] W. W. Cashin, The Fast Oxide Breeder – Fuel Irradiation Experiments, KAPL-1784 (August, 1957).

[4] J. D. Eichenberg *et al.*, "Effects of Irradiation of Bulk Uranium Oxide," Fuel Elements Conference, Paris, November 18-23, 1957, TID-7546, Book 2, pp. 616-716 (March, 1958).

[5] J. A. L. Robertson, A. S. Bain, and A. H. Booth, "Behavior of Uranium Oxide as a Reactor Fuel," The Second United Nations International Conference on the Peaceful Uses of Atomic Energy, Vol. 6, p. 655, United Nations, Geneva, Switzerland (1958).

of the pellets, have been postulated to explain this effect. In applications in which the external pressure is large enough to cause deformation of the cladding, as in the gas-cooled reactor, a further mechanism for disappearance of the gap is the collapsing of the thin-walled metal cladding about the fuel pellet.[6] Related to the disappearance of the radial gap in irradiation experiments is the appearance in many cases of a cylindrical central void, coaxial with the fuel pellet. Once again, various rationalizations of the observed behavior have been proposed. Regardless of the uncertainty of the mechanism, the observations are consistent in showing that the radial gap present during assembly disappears upon irradiation quite early in the exposure, after which the central temperatures reached by the UO_2 are independent of the initial gap over a wide range of gap dimensions.[3,4]

The lifetime of the metal-clad UO_2 fuel element is limited by the requirements that the tubing contain the fission products generated in the fuel body. As long as this condition is satisfied and the geometry of the fuel element is maintained within allowable tolerances, the element can continue to give satisfactory performance.[7] The exposure at which the element can no longer fulfill these criteria then determines the metallurgical lifetime of the fuel element. The most serious limitation on the lifetime may be the ability of the tube to contain the buildup of internal pressure due to the volatile fission products produced during the exposure. As the total amount of fission products released from the UO_2 fuel body increases, the pressure within the tubing will increase until it equals and eventually exceeds the external pressure of the coolant. From this point on, the most important factors determining the lifetime of the element are the creep-rupture properties of the fuel tubing and the rate of increase of the internal pressure. These and several other significant material problems related to the EGCR fuel element have been reviewed by Douglas.[8]

---

[6] J. P. Ellington, Creep Collapse of Tubes Under External Pressure, DEG Report, 162(R), (June, 1960).

[7] Fuel Life Prototype Enriched Gas-Cooled Power Reactor, IDO-24050 (February, 1959).

[8] D. A. Douglas, Jr., "Materials Research on Cladding for Gas-Cooled Fuel Element," Paper presented at Fuel Element Fabrication Symposium, Vienna, Austria, May 1960 (to be published).

Although data have been extracted from irradiation experiments and applied to the design of the EGCR, the dimensional and mechanical behavior of the EGCR fuel element needed to be firmly established. The following parameters are considered to be most important:

1. Axial expansion of the fuel pellets,
2. Radial expansion of the fuel pellets,
3. Fracture characteristics of the fuel,
4. The effect of rapid temperature excursions,
5. The integrity of the fuel capsule after thermal cycling, and
6. Thermal ratcheting of the fuel within the capsule.

An experimental apparatus[9] was designed that simulates the thermal conditions for the EGCR and has been utilized to study the dimensional behavior of the EGCR fuel element in an out-of-pile experiment. This report describes the data obtained using this rig during the dimensional studies program.

DESCRIPTION OF THE APPARATUS AND EXPERIMENTAL PROCEDURE

The equipment used for these experiments has been discussed in detail in a previous report.[9] The apparatus is shown pictorially in Fig. 2 and disassembled in Fig. 3. It has been possible to obtain maximum central temperatures of 4000°F in the fuel, rapid heating and cooling rates, and radial thermal gradients in the fuel pellet. Radiographic techniques were developed utilizing both x-ray and isotope radiation to permit observation of the fuel and cladding during testing.

The UO_2 pellet geometry is shown in Fig. 4. The pellets were prepared by sintering for 2 hr in a hydrogen environment at 3100°F to approx 95% of theoretical density. The length of each pellet was 0.750 in., while the height of the column of pellets in a single loading was 27 in. This column of pellets was loaded into a capsule simulating the geometry of the EGCR fuel element and the expansion behavior was observed at temperature by means of low-voltage radiography using a 250-kvp x-ray machine. The x-ray procedure has been previously discussed.[9] This technique permitted measurement and observation of both

[9] W. R. Martin and J. R. Weir, A Device to Simulate the Service Thermal Conditions in EGCR-Type Fuel Elements, ORNL-3032 (December 28, 1960).

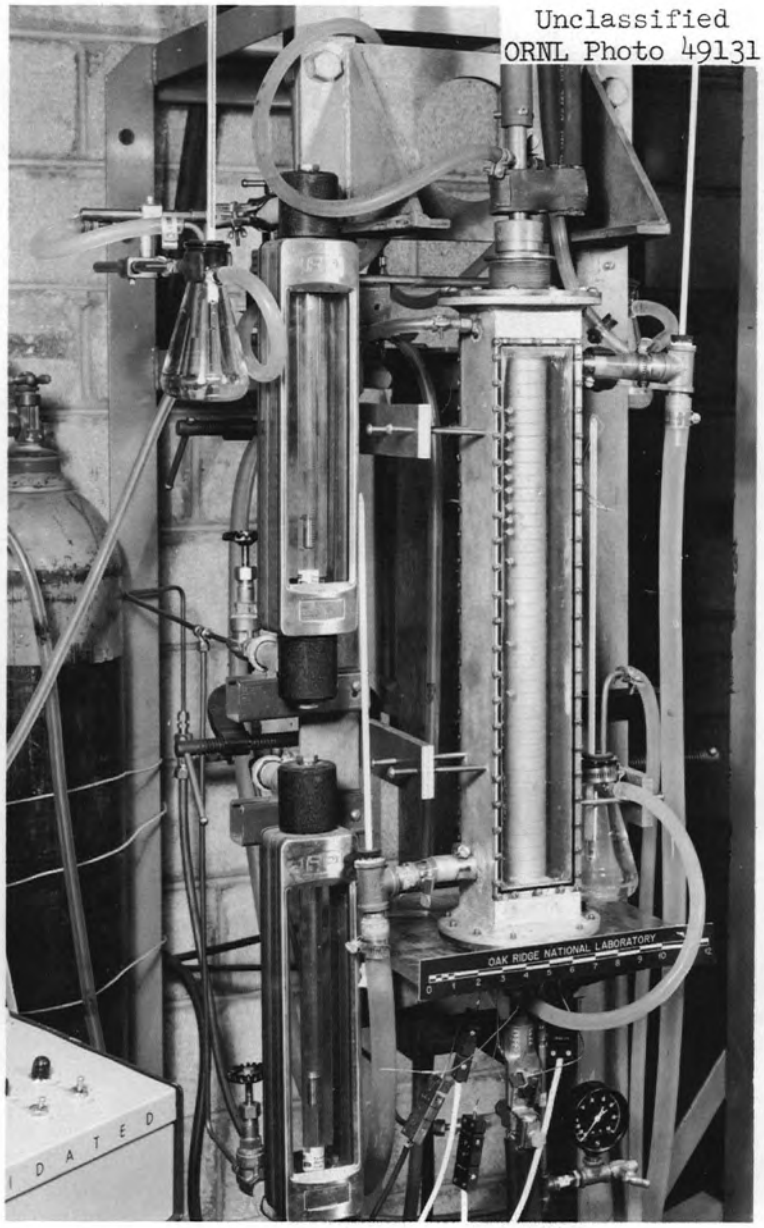

Fig. 2. Experimental Apparatus.

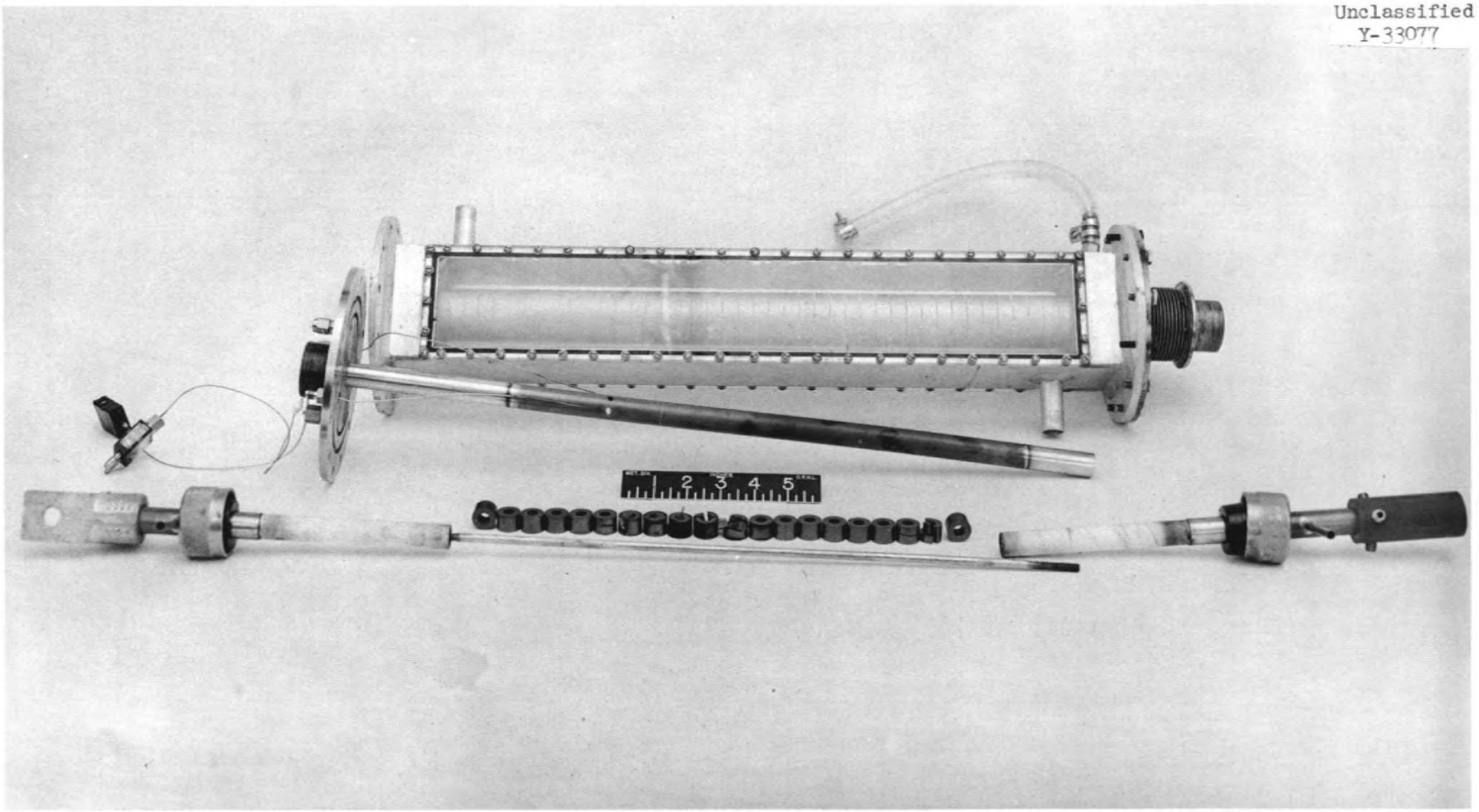

Fig. 3. View of Disassembled Apparatus.

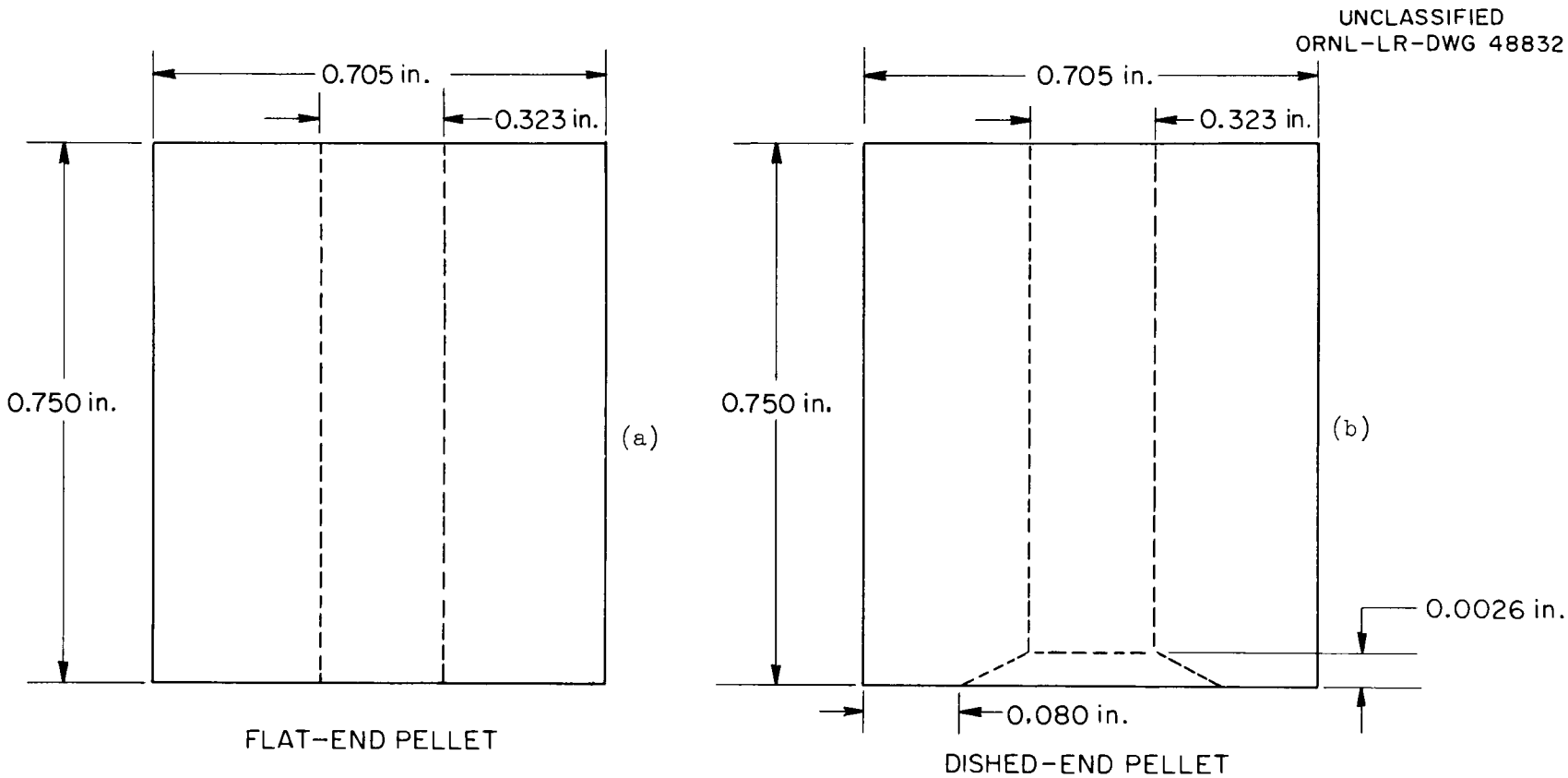

Fig. 4. Geometry of Dished and Flat End Pellets.

the axial and radial expansion characteristics of the fuel capsule and also the relative growth of the components. Gamma radiography, using the Ir^{192} isotope, was used to observe crack formation in the UO_2 at the elevated temperatures.

The position of the UO_2 pellets was observed at room temperature and at increments of 500°F up to a central temperature of 3000°F. The radial temperature gradients in the fuel capsule at steady-state conditions for various central temperatures are shown in Table 1.

Table 1. Radial Thermal Gradients in Capsule Simulating the EGCR Fuel Element

Central UO_2 Temperature (°F)	Average Cladding Wall Temperature (°F)	Average Temperature Gradient (°F)
1000	785	215
1500	1160	340
2000	1385	615
2500	1520	980
3000	1705	1295

The axial temperature profiles for several temperature levels are shown in Fig. 5. Radiographs of the capsule were taken to determine the expansion of the fuel at various steady-state temperature conditions. The radiographs were then projected on a screen to a magnification of 25X. Appropriate measurements were made at this magnification and compared to standards so that changes in dimensions of the order of one thousandth of an inch could be determined.

The fuel element behavior program was separated into two parts. First, the dimensional behavior of the capsule was observed when a radial gap existed between the cladding and the fuel pellet. Secondly, the behavior was observed after the cladding had been collapsed around the pellet by means of external pressure. In the latter case, no radial gap existed between the pellets and the cladding during the test.

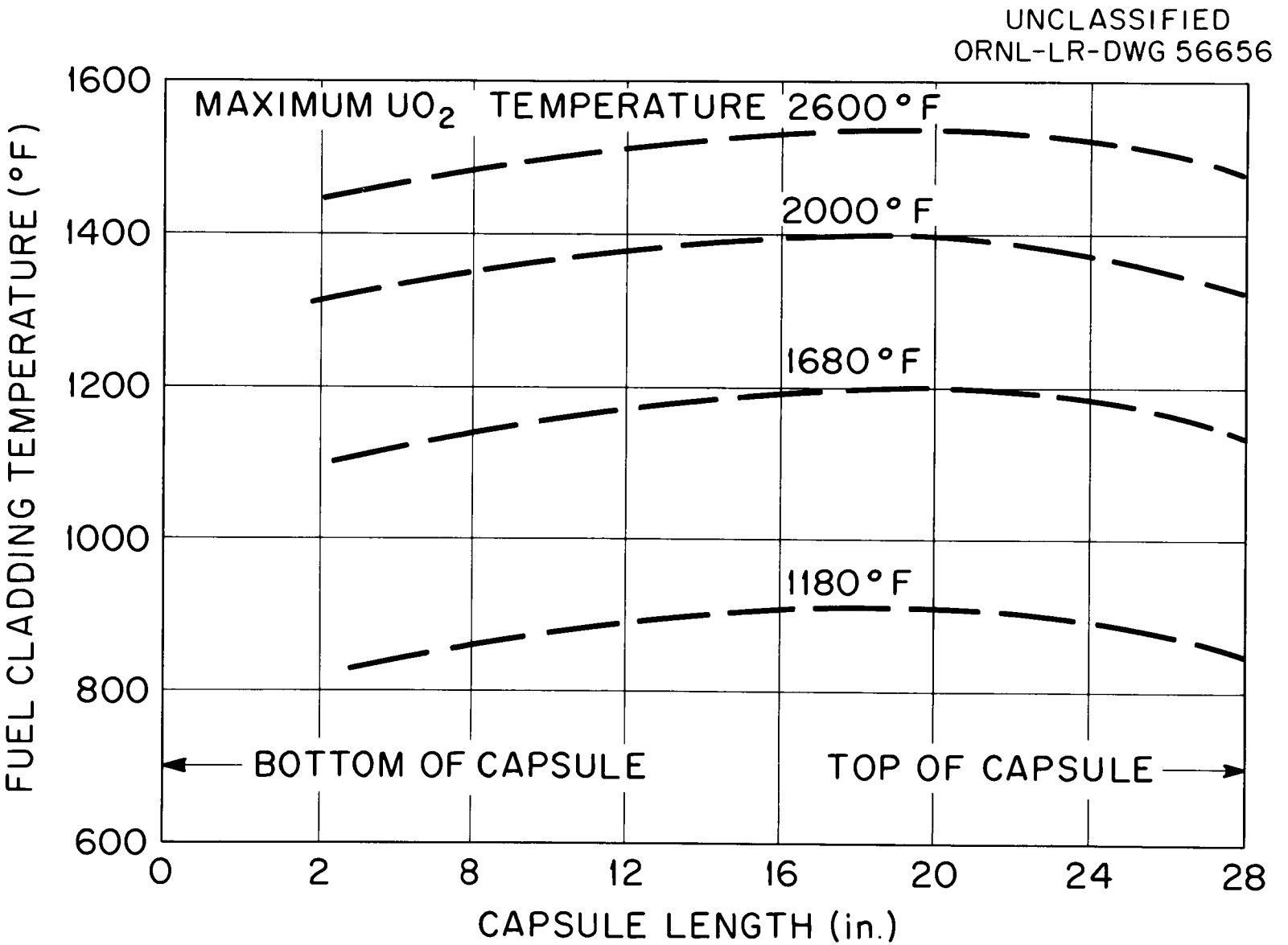

Fig. 5. Axial Temperature Distribution for Simulated EGCR Fuel Element.

A modified version of the device described previously[9] was constructed to allow a gas pressure differential up to 325 psi to be applied to the fuel capsule. This permitted the collapsing behavior of the cladding to be observed while the fuel within the capsule was subjected to thermal conditions similar to those predicted for the EGCR. The pellets were loaded into the apparatus and heated to a given temperature with a pressure differential applied to the capsule. The extension of the pellet and cladding was observed at successive temperature levels during the initial heating period. In addition, periodic radiographic measurements were taken at the maximum temperature. The capsule was held at the elevated temperature until the cladding had collapsed sufficiently to allow contact between the capsule wall and the UO_2.

The investigation of the behavior of the capsule during thermal cycling was performed in two parts. First, the thermal-cycling behavior was observed for capsules which had an 0.003- to 0.007-in.-diametral gap upon assembly and secondly, for those capsules in which the cladding had been collapsed around the pellets by external gas pressure. The average cladding heating and cooling rates were 150°F/min with a maximum of 250°F/min and a minimum of 100°F/min. The maximum and minimum UO_2 temperatures during these tests were 2800 and 400°F, respectively. Both radiographic and electronic methods were utilized for measurement of the cladding elongation during cycling. The modification of the basic apparatus to allow for the second method of measurement is shown in Fig. 6. The capsule temperature was cycled between upper limits of 1300 to 1600°F and lower limits of 340 to 1100°F.

PART I. DIMENSIONAL BEHAVIOR OF CAPSULE WITH RADIAL GAP BETWEEN CLADDING AND FUEL

Thermal Expansion of UO_2

The thermal expansion of the pellets (Fig. 4) is very nearly a function of the central UO_2 temperature. Axial expansion data obtained are plotted in Fig. 7 along with values of expansion calculated from isothermal dilatometer test

UNCLASSIFIED
ORNL-LR-DWG 56207

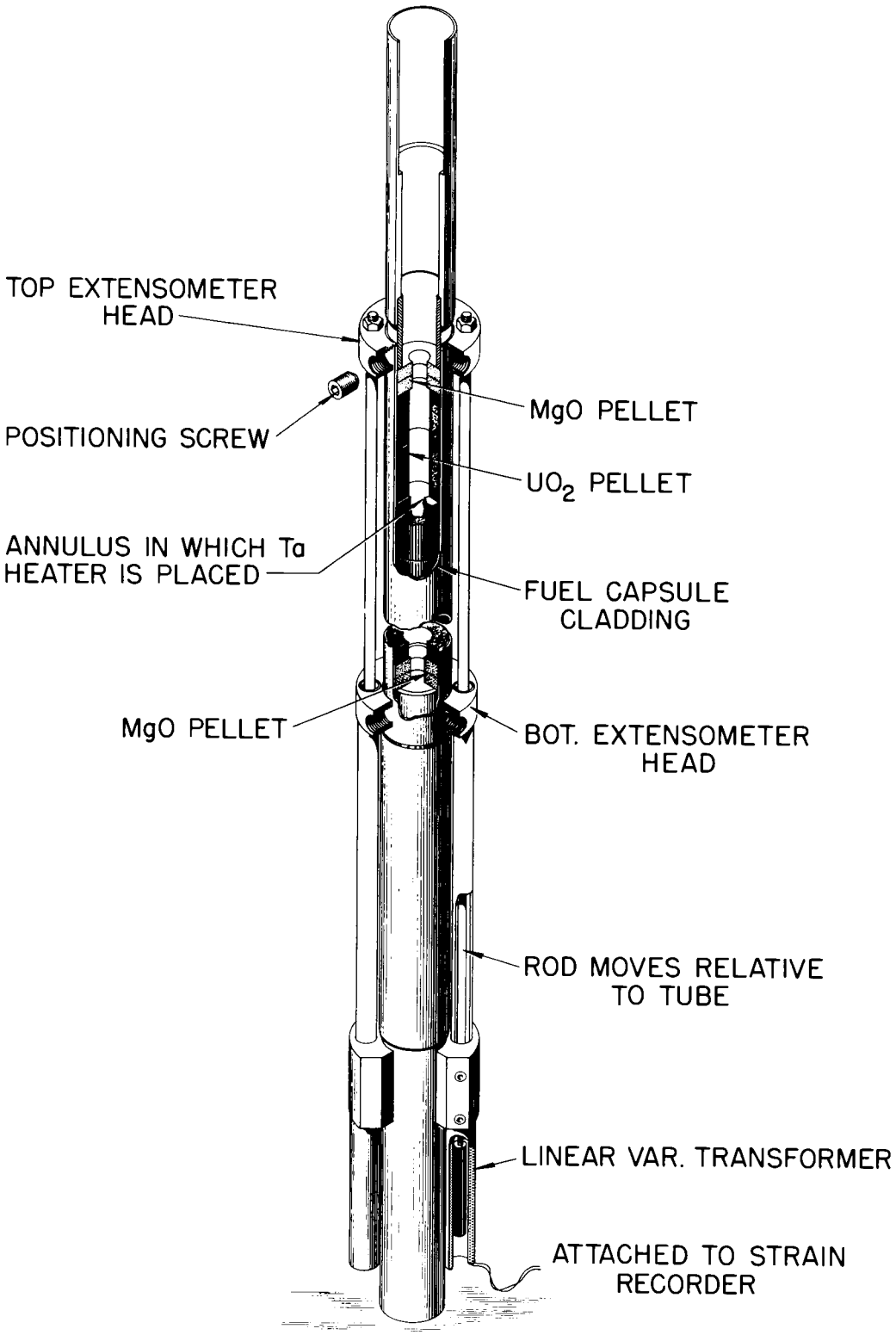

Fig. 6. Extensometer for Measurement of Axial Elongation of Simulated EGCR Fuel Element.

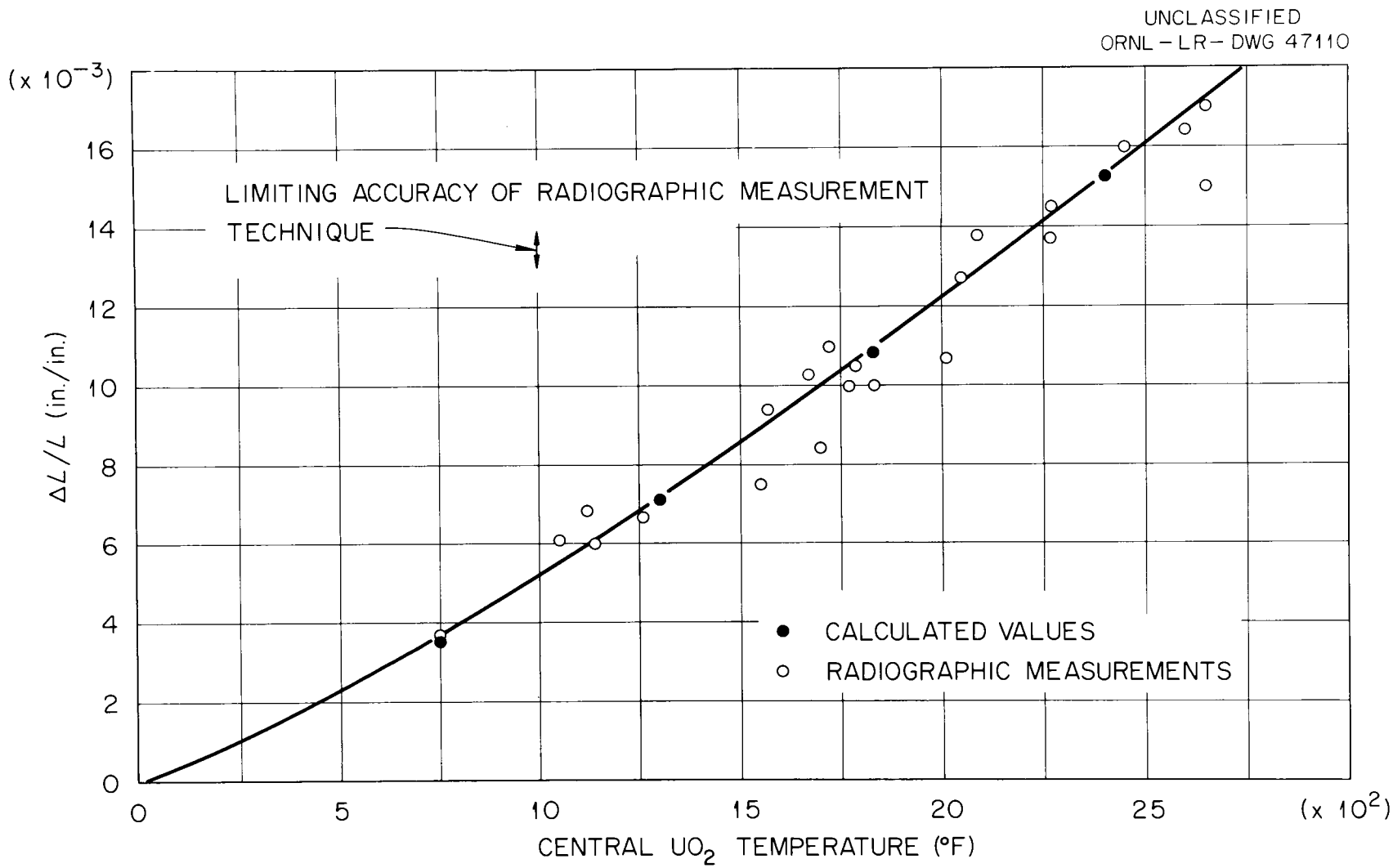

Fig. 7. Expansion Behavior of 95% Theoretical Density UO_2 Pellets with Radial Thermal Gradients.

results.[10] It is concluded from this plot that the expansion is a function of the inner surface temperature of the pellet rather than a mean temperature. Further evidence that the column height is a function only of the central temperature is the observation that for a central temperature of 1256°F a temperature gradient of either 275 or 375°F results in equivalent column heights. As the radial thermal gradient is increased, the contact area between adjacent pellets is reduced. This is shown clearly for a central temperature of 3000°F in Fig. 8. This observation is further evidence that the axial expansion of the pellets is a function of the central temperature. Cylindrical UO_2 pellets of 70% theoretical density were subjected to temperature transients by other investigators.[11] The UO_2 exhibited a positive linear coefficient of expansion of approximately the same magnitude as that reported for UO_2 bodies measured under isothermal conditions.

A modification, called dishing, of the pellets was made to investigate the possibility of decreasing the axial expansion of the UO_2 column within the cladding. A sketch of the new geometry is shown in Fig. 4b. A summary of the results for pellets dished on one end is compared to the axial expansion of flat end pellets in Table 2. The axial expansion is reduced appreciably only at the higher temperatures or at a point where the radial thermal gradient becomes quite large.

Table 2. Axial Expansion of 95% Theoretical Density UO_2 Pellets (in./in.)

	Maximum Central UO_2 Temperature (°F)				
	1000	1500	2000	2500	2750
Regular pellets	0.0050	0.0083	0.0122	0.0162	0.0183
Dished pellets (one end only) Average bevel 0.00257	0.0053	0.0081	0.0112	0.0142	0.0159

[10] S. D. Fulkerson, Apparatus for Determining Linear Thermal Expansions of Material in Vacuum or Controlled Atmosphere, ORNL-2856, p. 35 (December 21, 1959).

[11] W. C. Cohen and D. F. Molina, Behavior of UO_2 Bodies Subjected to Temperature Transients, KAPL-1873 (July, 1957).

UNCLASSIFIED
ORNL-LR-DWG 45981

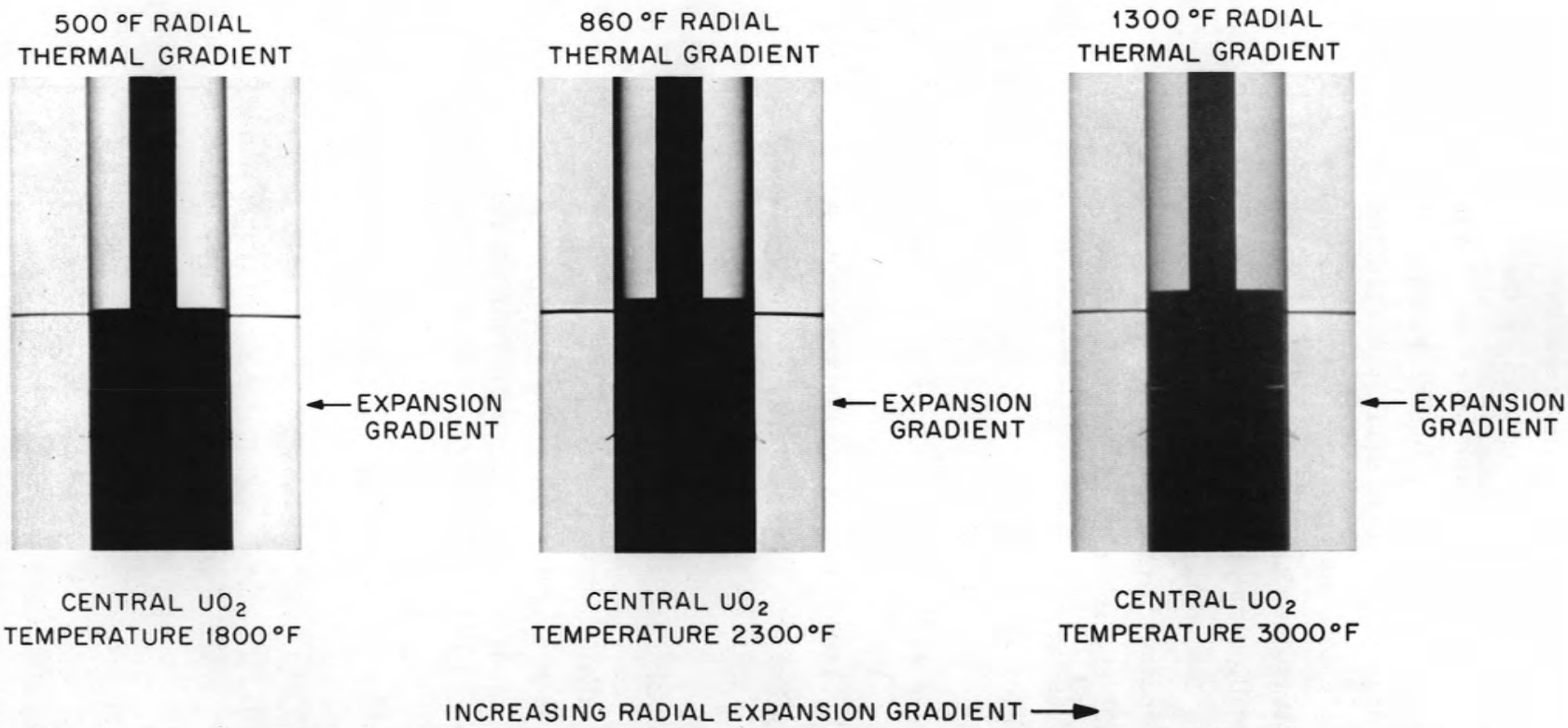

Fig. 8. Expansion Profile of UO_2 Pellets in Simulated EGCR Fuel Capsule.

Pellets with both ends dished were also tested. The amount of chamfer on each end was the same for these pellets as the chamfer on the pellets dished on one end only. The axial expansion behavior of double-dished pellets is the same as the expansion characteristics of the single-dished pellets. The contact points between adjacent pellets will establish the axial expansion of a stack of pellets. The expansion profile of a single fuel pellet is a function of the temperature distribution in that pellet. Because of the radial temperature distribution in the UO_2, the area of contact between adjacent pellets will be located near the inside diameter of the fuel pellet. When one end of a pellet is dished, the contact area between adjacent pellets is moved toward the cooler region in the UO_2 and hence reduces the total axial expansion of a stack of pellets. It is assumed that the contact area is not shifted significantly closer to the outer surface of the fuel by double dishing the ends of the fuel pellet.

The effective radial expansion is also very nearly a function of central UO_2 temperature. The pellets expand radially as a solid pellet until they are at approx 1200 to 1300°F at which time the ΔT is 275°F. At this point, large radial cracks appear as shown in Fig. 9a and the pellet expands through opening of these cracks.

Thermal Expansion of Type 304 Stainless Steel

Thermal expansion of type 304 stainless steel was determined by isothermal dilatometer tests and by radiographic techniques in the thermal simulation apparatus. The results as presented in Table 3 agree favorably with other mean coefficients of linear expansion found in the literature.

Thermal Expansion of the Fuel Capsule

The axial expansion of the fuel capsule was found to be the same as if the fuel and cladding were subjected to these thermal conditions and tested separately. As expected, the pellets crack radially upon heating and expand until the pellet makes contact with the inner surface of the cladding. In this manner, the pellet contacts the cladding at three points on the circumference. Thus, the radial gap

Unclassified
Y-33895

(b) Room Temperature

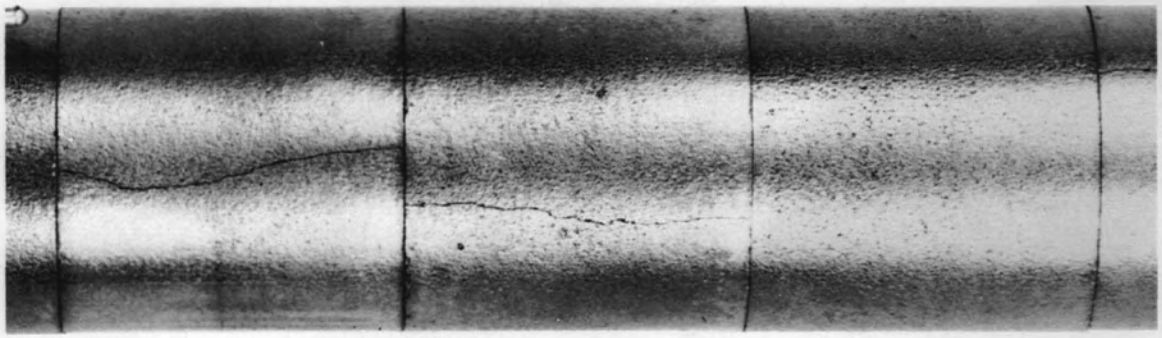

Unclassified
Y-37296

(a) Elevated Temperature

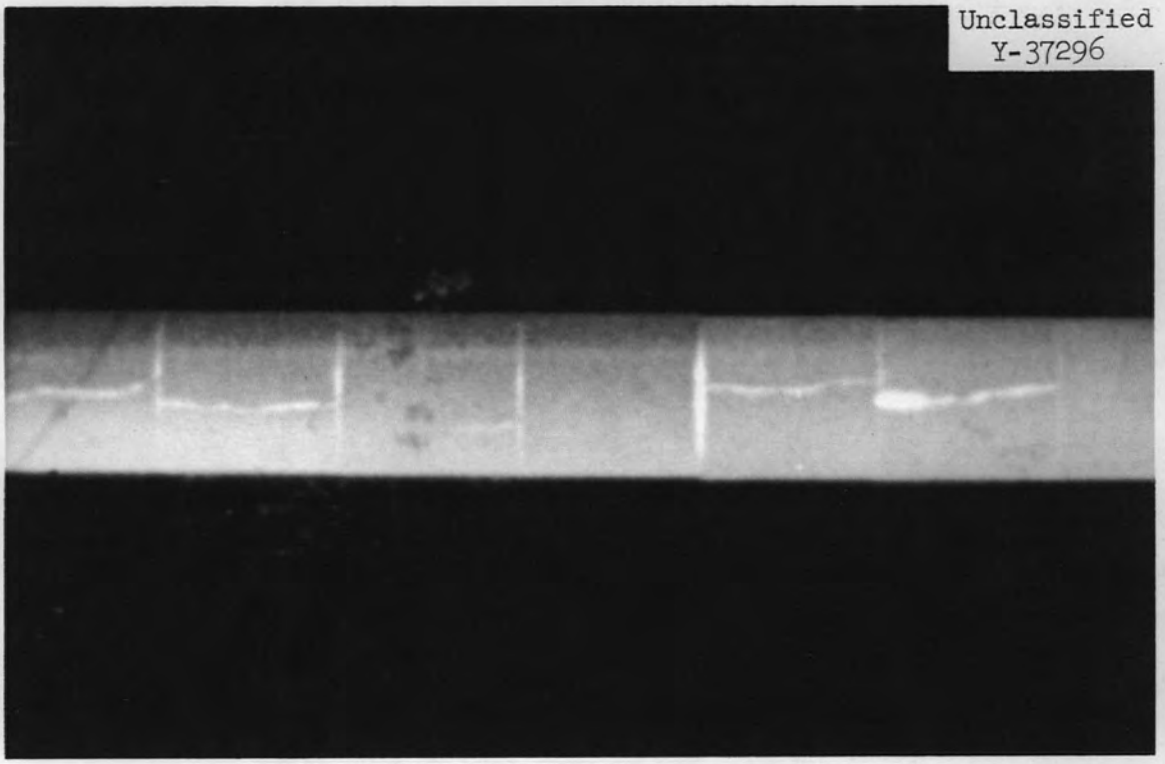

Fig. 9. Radial Cracks in Fuel at Room and Elevated Temperatures.

Table 3. Coefficient of Linear Expansion of Type 304 Stainless Steel
Mean Coefficient x 10^6 per °F

°F Range	Alpha	Alpha-9*	Alpha-10**
100–500	9.9	9.5	9.5
100–1000	10.3	10.0	10.4
100–1600	10.7	--	--

*D. E. Furman, "Thermal Expansion Characteristics of Stainless Steel," Trans. Met. Soc. AIME, 188 (May, 1951).

**J. B. Austin and R. H. H. Pierce, "Thermal Expansion of Heat Resisting Iron Alloys," Ind. Eng. Chem., 25, 776 (1933).

at temperature varies from zero to a value that is a function of the relative radial expansion between pellet and cladding. In these tests the latter value was found to be approximately the same as the diametral gap present after assembly. The contact between pellet and cladding formed by cracking and expansion of the fuel pellets did not affect the axial expansion of either component.

Behavior of the Capsule During Thermal Cycling

The capsules were thermal cycled between cladding-temperature limits of 500 and 1500°F with no detectable change in expansion characteristics of either the cladding or fuel as long as the radial gap existed between the fuel and the cladding. This is true even when the pellets have fractured radially and make contact with the cladding. These observations are consistent with those obtained during a single heat-up period.

The powder fines resulting from the fractured UO_2 did not exceed 0.0005% of the total weight per thermal cycle.

Fracture Characteristics of the Fuel Pellet

Typical pellets after exposure to thermal cycling and removal from the cladding are shown in Fig. 10. The cracks have been viewed both at room temperature (Fig. 9b) and at elevated temperatures (Fig. 9a). The types of pellet fracture fall into three categories. Further, the development of the cracks occurs in three stages. A drawing showing the various modes of fracture is shown in Fig. 11. Typical microstructures of fractured UO_2 pellets in Figs. 12a and 12b show the micro- and macrocracks in the UO_2 fuel pellets. The microcracks are seen to be both intergranular and transgranular. A cross section of a capsule after a typical test is shown in Fig. 13. The radial cracks are first visible in the fuel at a central temperature of 1250°F at which time the ΔT is 275°F. The fracture stress of the pellet from thermal stress was calculated[12] to be 35 800 psi at 1250°F. It is probable that the crack was initiated at a lower stress and a ΔT of 275°F was required to propagate the fracture through the pellet.

[12] W. D. Kingery, "Thermal Stress Resistance," Property Measurement at High Temperatures, p. 185, John Wiley and Sons, Inc., New York, 1955.

Unclassified
Y-34599

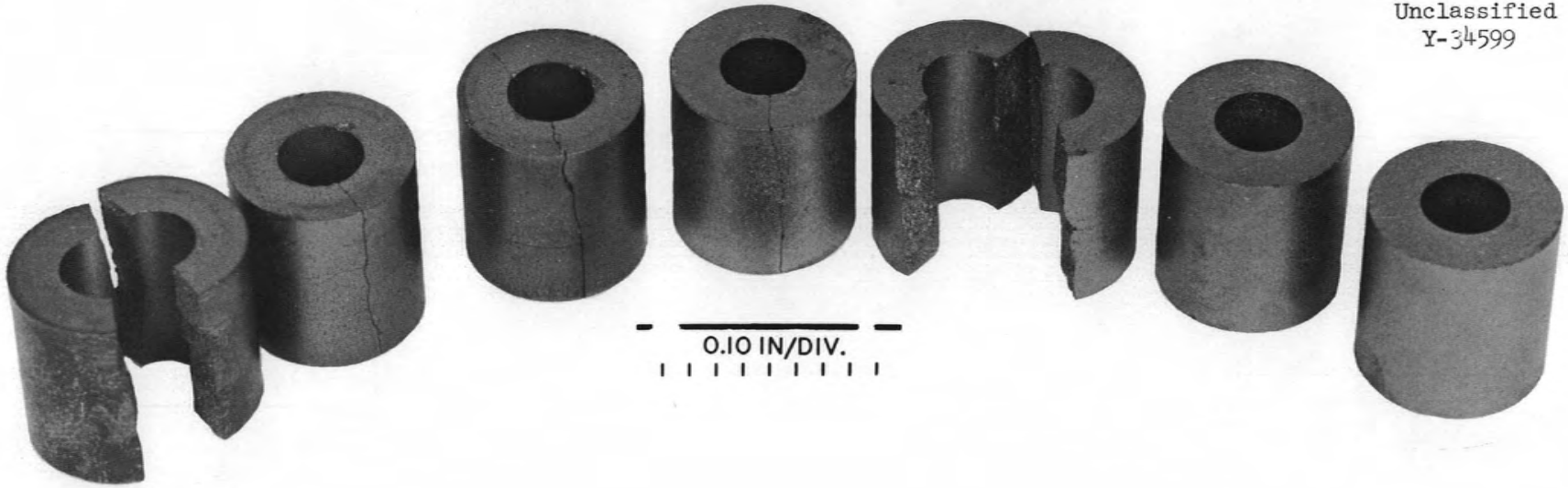

Fig. 10. Uranium Dioxide Pellets After Test in Simulated EGCR Fuel Capsule.

UNCLASSIFIED
ORNL-LR-DWG 46932

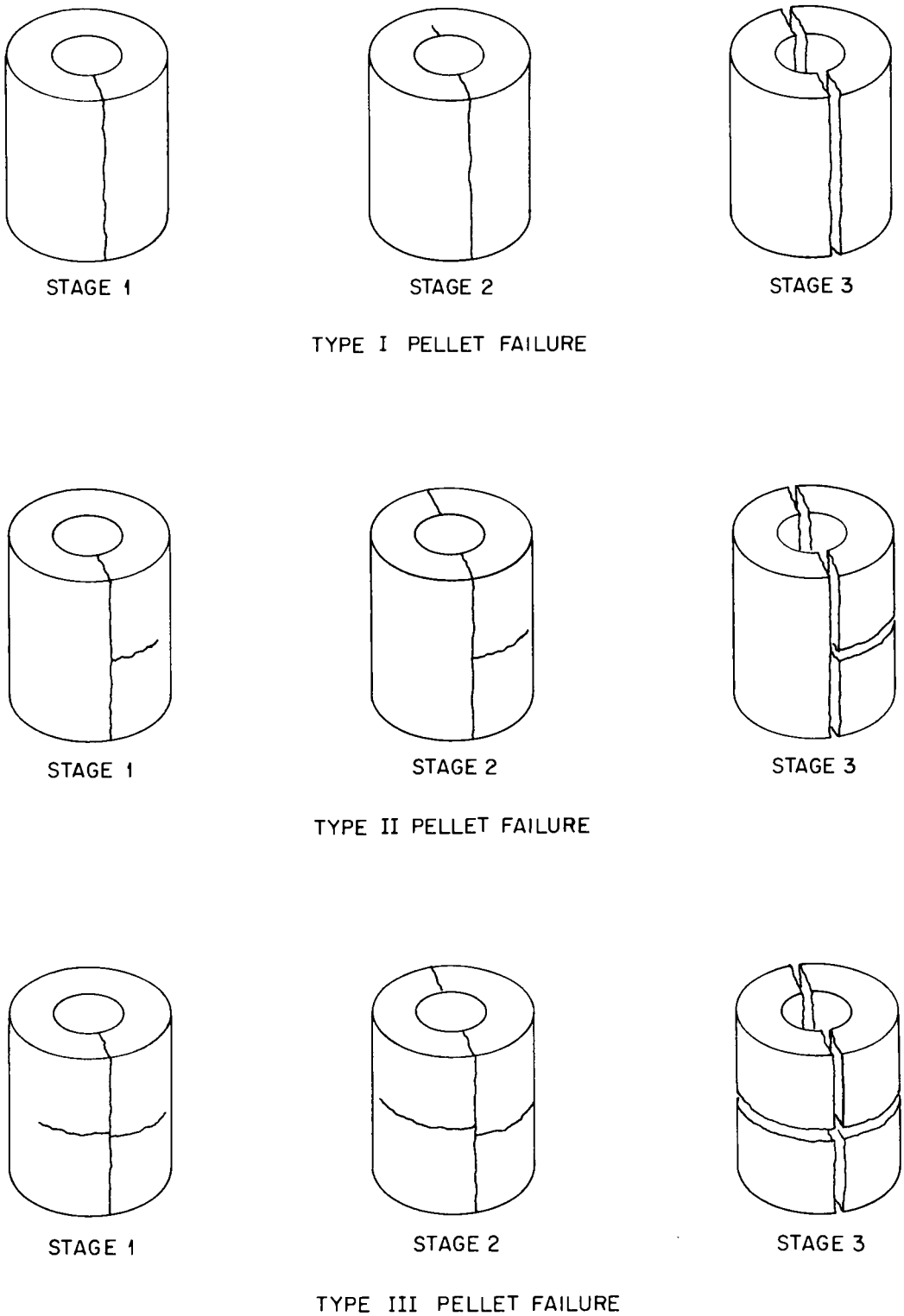

Fig. 11. Types of Pellet Failure by Fracture.

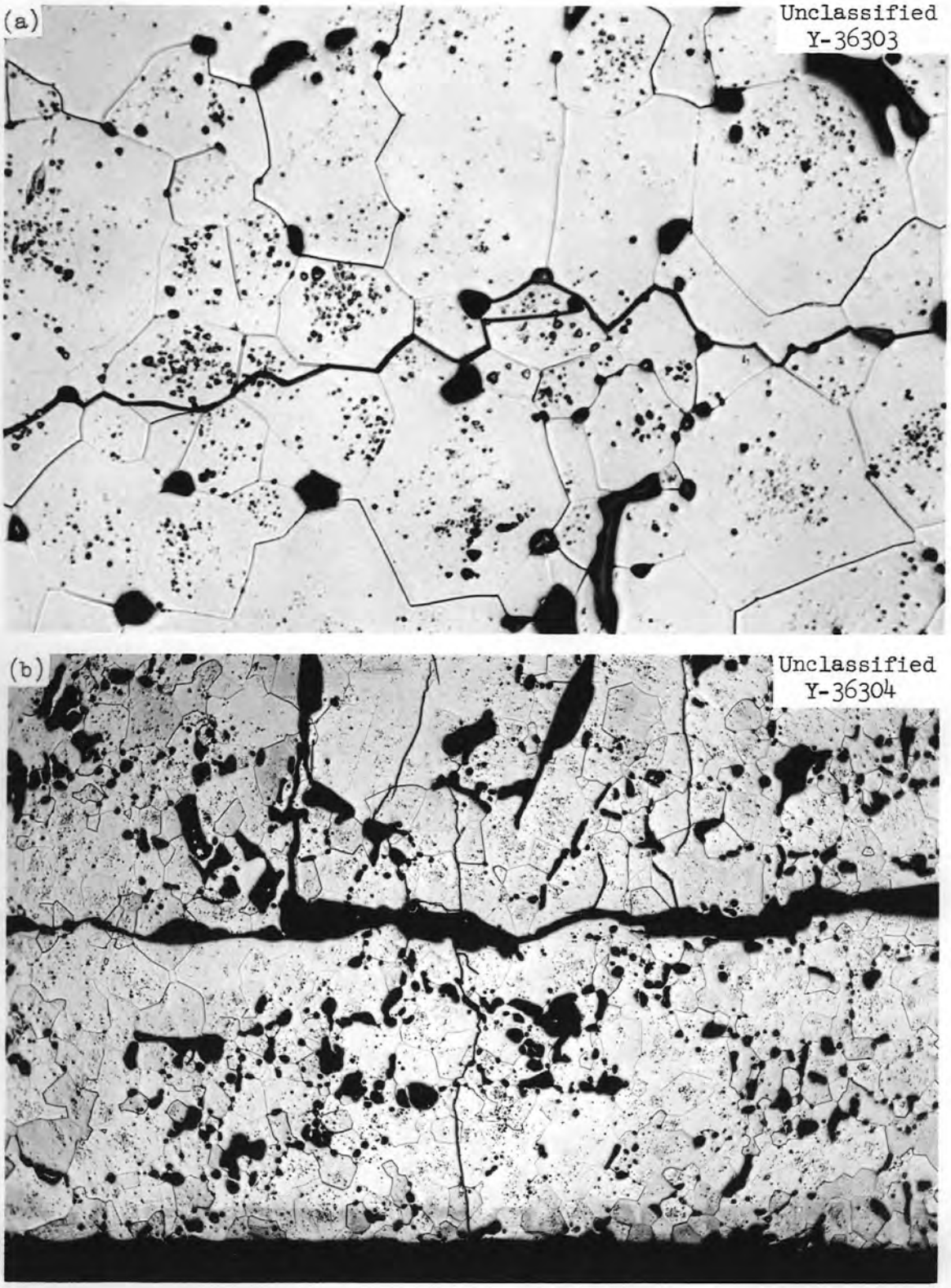

Fig. 12. (a) Microstructure of UO_2 Showing Microcracks both Transganular and Intergranular, 500X, (b) Microstructure of UO_2 Showing Macro- and Microcracks, 100X.

Unclassified
Y-34840

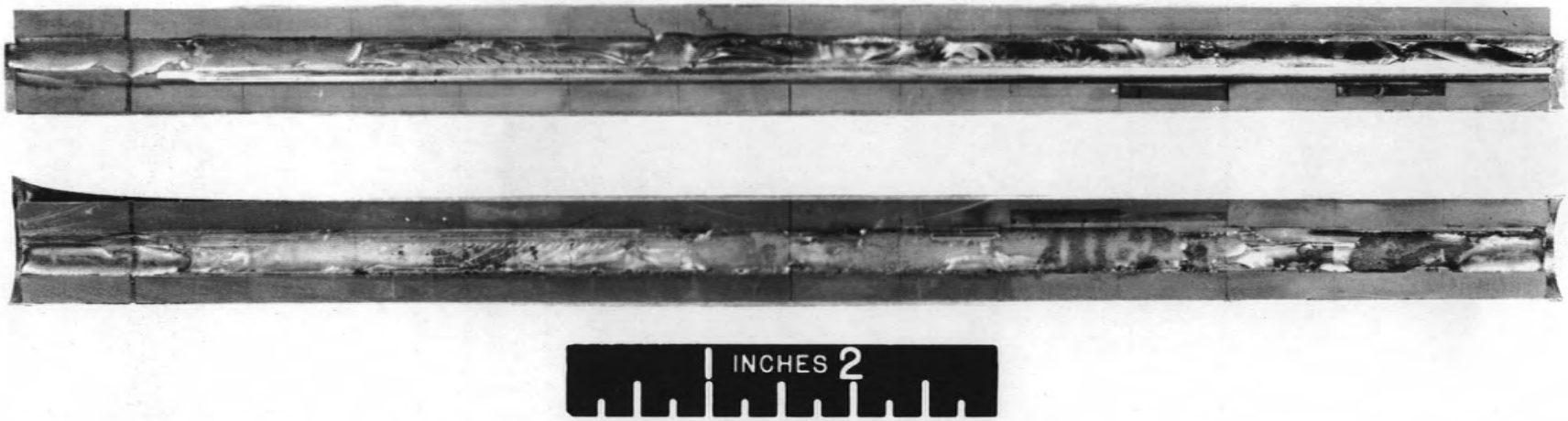

Fig. 13. Simulated EGCR Fuel Capsule Sectioned After Injection Hardening Experiment.

Total Surface Area Measurements of UO_2

The total surface area of the pellets shown in Fig. 10 was measured by the BET method. The results are listed in Table 4. From these data one might

Table 4. Total Surface Area of 2.6% Enriched (95% Dense) UO_2 EGCR Pellets

Condition of Pellet*	Total Surface Area M^2/Pellet
AFTER TEST	
Pellet 1, discolored surface	0.831
Pellet 2, (1) radial plus (1) circumferential crack	0.175
Pellet 3, (1-3/4) radial cracks	0.141
Pellet 4, (1) radial crack	0.099
Pellet 5, (2) radial cracks	0.154
Pellet 6, no macrocracks	0.055
BEFORE TEST	
Pellet 7, no macrocracks	0.079

*At time of surface area measurements.

conclude the total surface area is dependent upon type and number of macrocracks and the nature of the oxide surface. However, it also may be postulated that the total surface area is an indication of the pellet's tendency to crack; that is, the pellets with a higher total surface area may crack more readily than those with a lower total surface area. During these experiments it was observed that one pellet might crack under given temperature conditions while its nearest neighbor at the same temperatures would not crack. Therefore, the total surface area of each pellet in a second group of ten was measured both before and after a simple thermal-cycle treatment. These results indicated no apparent correlation between the total surface area of a pellet in the as-sintered condition before thermal cycling and its tendency to fracture at elevated temperatures during thermal cycling. Furthermore, the number of macrocracks in only five of the ten pellets correlated with the change in total surface area after test. Typical microstructures of UO_2 pellets are found in Fig. 14.

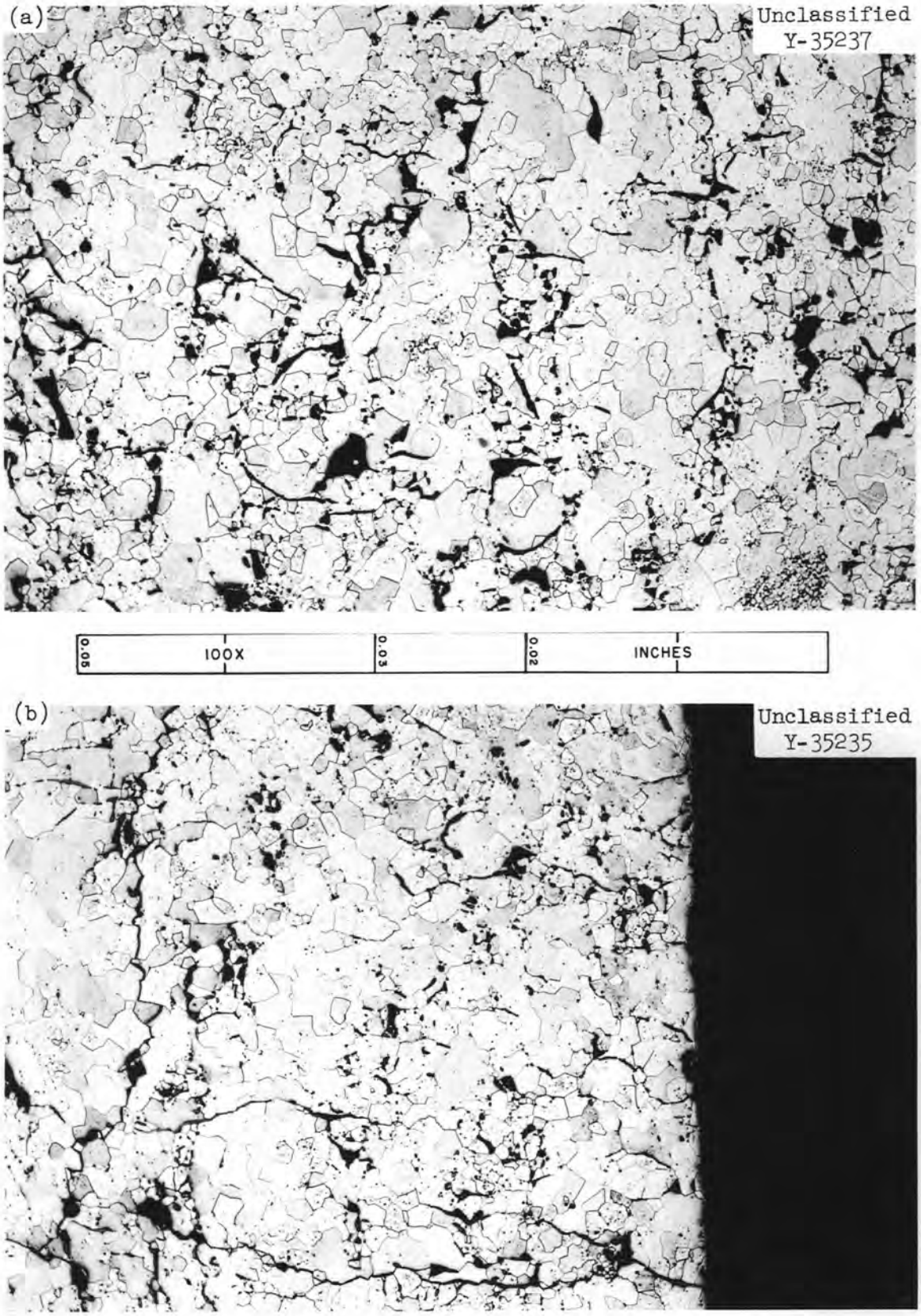

Fig. 14. (a) Typical Microstructure of UO_2 at 0.270-in. Radius, (b) Typical Microstructure of UO_2 at 0.350-in. Radius, 100X.

PART II. DIMENSIONAL BEHAVIOR OF SIMULATED EGCR FUEL ELEMENT WITH NO RADIAL GAP BETWEEN CLADDING AND FUEL PELLET

The dimensional behavior of the simulated fuel element during thermal cycling while the cladding material is exposed to a 300-psi pressure differential is quite different from the behavior in those tests in which no pressure differential exists. The expansion of the pellets before the cladding collapsed about the UO_2 pellets was very nearly a function of the central UO_2 temperature. After the cladding has collapsed sufficiently to allow contact between pellet and cladding, very different results are obtained during thermal cycling.

Collapse of Cladding About Fuel

The cladding may be collapsed by external pressure with the UO_2 in one of two initial thermal conditions. In the first case, the cladding and UO_2 are at the same temperature. In the second case, the cladding temperature is in the neighborhood of 1500°F with a central UO_2 temperature of 2500°F. Regardless of which thermal situation is employed, the visible condition of the fuel capsule after collapse is essentially the same.

A capsule with an 0.005-in.-diametral gap between cladding and UO_2 was heated to an isothermal temperature of 1900°F and held for 12 hr under external pressure. The results of this collapsing treatment are shown in Fig. 15. Note the formation in the cladding of circumferential ridges which correspond to the position of the interface between pellets within the capsule. Also note the shape of the collapsed tube above the top pellet. There was no clearance between the top pellet and the end plug before the capsule was heated. The end plenum of 0.125 in. at elevated temperature was entirely a result of the differential expansion between cladding and UO_2.

Thermal Cycling of Capsule with no Radial Gap

This capsule was then heated and thermal cycled with no pressure differential across the capsule wall. A malfunction in the testing apparatus prevented accurate

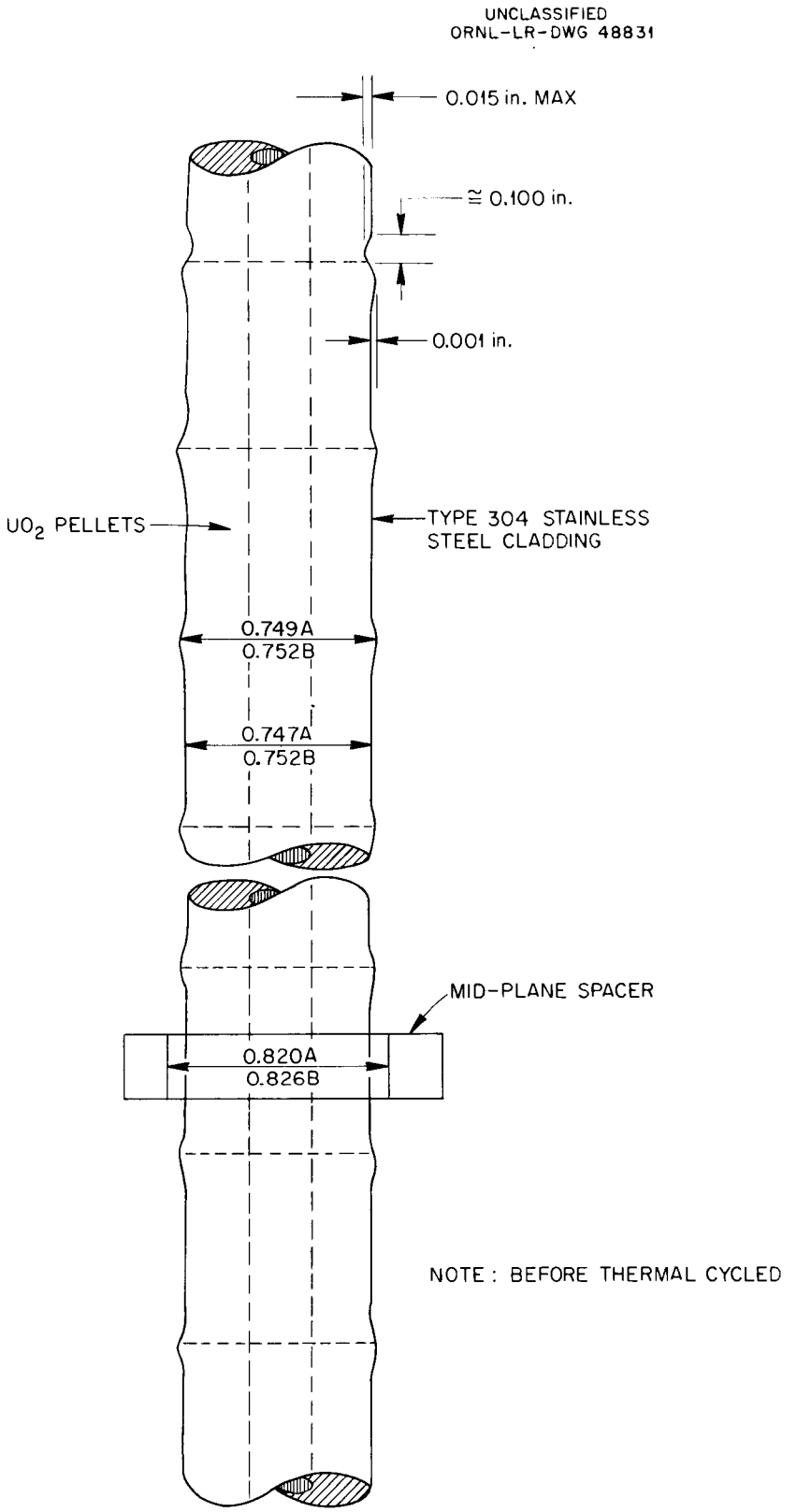

Fig. 15. Simulated EGCR Element Collapsed at Isothermal Conditions.

dimensional measurements during the experiment. However, the expansion was not singularly dependent upon cladding or UO_2 central temperature, but rather dependent upon both of these parameters in addition to the number of thermal cycles. Gaps appeared between pellets during thermal cycling. The shape and the dimensions of the buckled area in the cladding above the top pellet did not change appreciably during thermal cycling. After test, measurements disclosed that the collapse was not uniform in either the area above the top pellet or along the axis of the capsule. The microstructure of the cladding in the area of the top plenum is shown in Fig. 16.

A more realistic capsule collapse is obtained if the cladding is collapsed about the UO_2 while the fuel is subjected to thermal conditions simulating those predicted for the EGCR (i.e., radial thermal gradients and high UO_2 central temperatures).

Initially a capsule was subjected to an external pressure of 320 psi for 32 hr during which the average cladding temperature was 1420°F and the central UO_2 temperature was 2350°F. At these conditions, the cladding collapsed sufficiently to permit contact between the cladding and UO_2 in 30 hr. This capsule was then thermally cycled through 109 cycles between temperature limits of 400 and 1475°F on the cladding with a 300-psi-helium pressure differential applied. The results of this test revealed the following:

1. The relative position of the top UO_2 pellet and stainless steel cladding did not change during the 109 cycles.
2. The total permanent axial strain introduced in the cladding was 0.45%.
3. Gaps were formed between each of the UO_2 pellets. Some of these were as large as 0.020 in.
4. Circumferential ridges were formed in the cladding at positions which correspond to interfaces between pellets, but the ridges were not large enough to be measured by a commercial shadowgraph technique.

Following examination, this capsule was returned to the testing equipment and held at cladding and central UO_2 temperatures of 1550 and 2750°F, respectively. After 65 hr at these conditions, the cladding had collapsed so that it conformed very closely to the "hourglass" profile of the UO_2 pellets. The capsule was cycled between central UO_2 temperatures of 400 and 2750°F for 48 cycles.

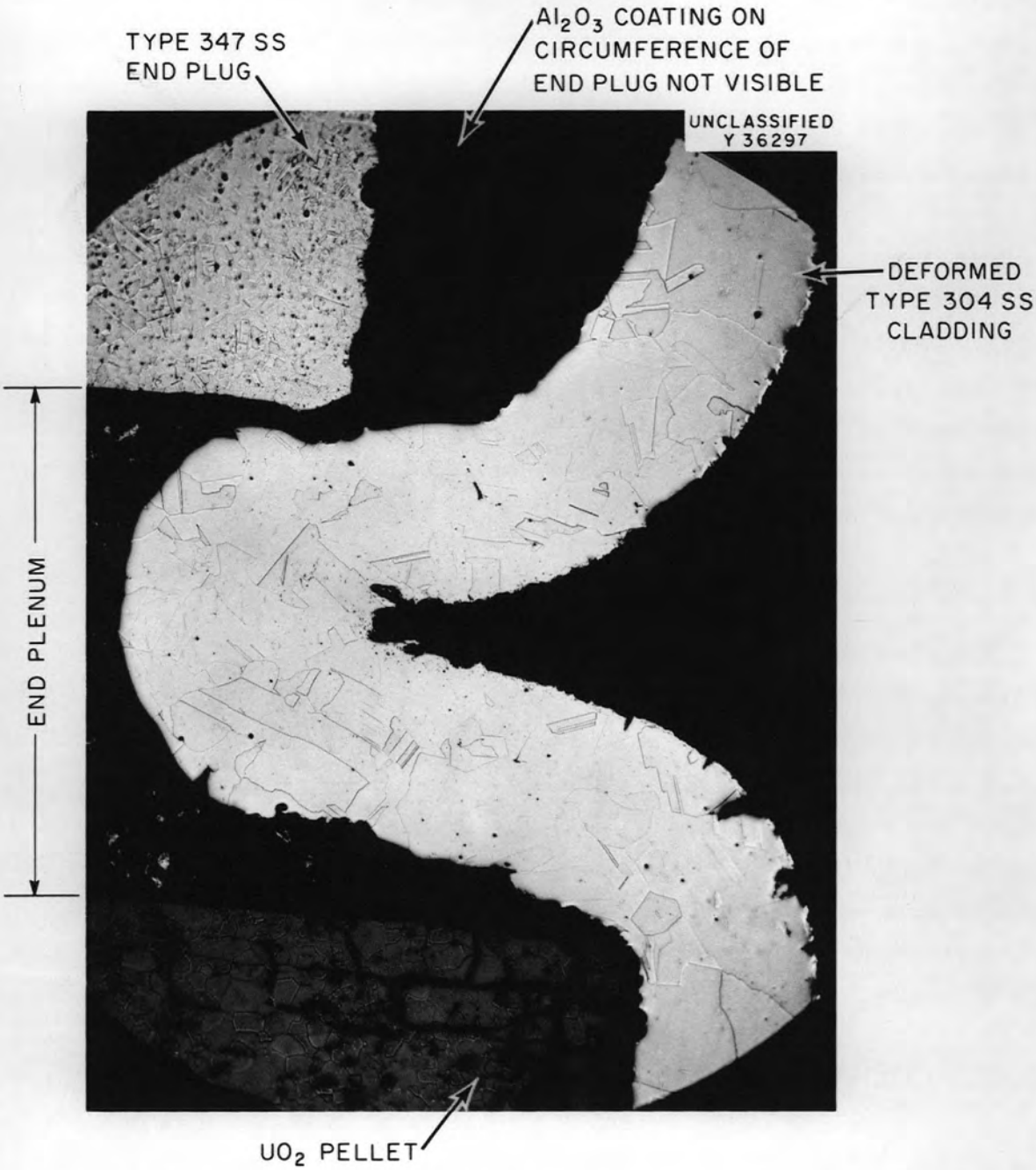

Fig. 16. Magnification of Collapsed Cladding into End Plenum of Capsule Collapsed at Isothermal Conditions. No end plenum existed in the as-assembled condition.

The data and post-test examination revealed that the dimensional characteristics of the capsule changed markedly during thermal cycling. The gaps between the pellets grew with successive cycling and openings as large as 0.040 in. were observed. The total elongation of the cladding was 2.5% after this second test.

The capsule was placed in the test rig a third time to determine whether the cladding would collapse into the gaps between the pellets. This did not occur after 330 hr at a cladding temperature of 1550°F.

The thermal-cycling results at peak cladding temperatures of 1420°F and higher were analyzed after several additional experiments similar to those described above. At a given temperature, the permanent axial strain measured after test in the cladding was assumed to be a linear function of the number of thermal cycles. Therefore, for a given peak cladding temperature, the plastic strain per cycle, ϵ_p/n, could be calculated. The results indicated that a relationship between ϵ_p/n and temperature might exist.

Investigation of Axial Extension of Capsule During Cycling

To further investigate this growth phenomenon, the axial elongation during cycling was then electronically measured by means of an extensometer and micro-former arrangement. A photograph of the simulated fuel element before and after test is shown in Fig. 17. This technique of measurement permitted a more detailed investigation of the axial elongation phenomenon than was possible using radiographic techniques. Through the use of this extensometer, it was confirmed that thermal cycling a capsule with a diametral gap between fuel and clad at elevated temperatures results in no permanent axial elongation. Typical plots of extension versus number of thermal cycles are found in Fig. 18.

After the cladding had been collapsed about the fuel, the capsule was again thermal cycled. The resultant axial elongation rate during cycling is shown in Fig. 19. The results indicate that the total elongation is a linear function of the number of cycles.

It is therefore concluded that one necessary criterion for axial growth of the fuel capsule is the absence of the diametral gap between fuel and cladding. Further, from the results of the experiment in which the cladding was collapsed

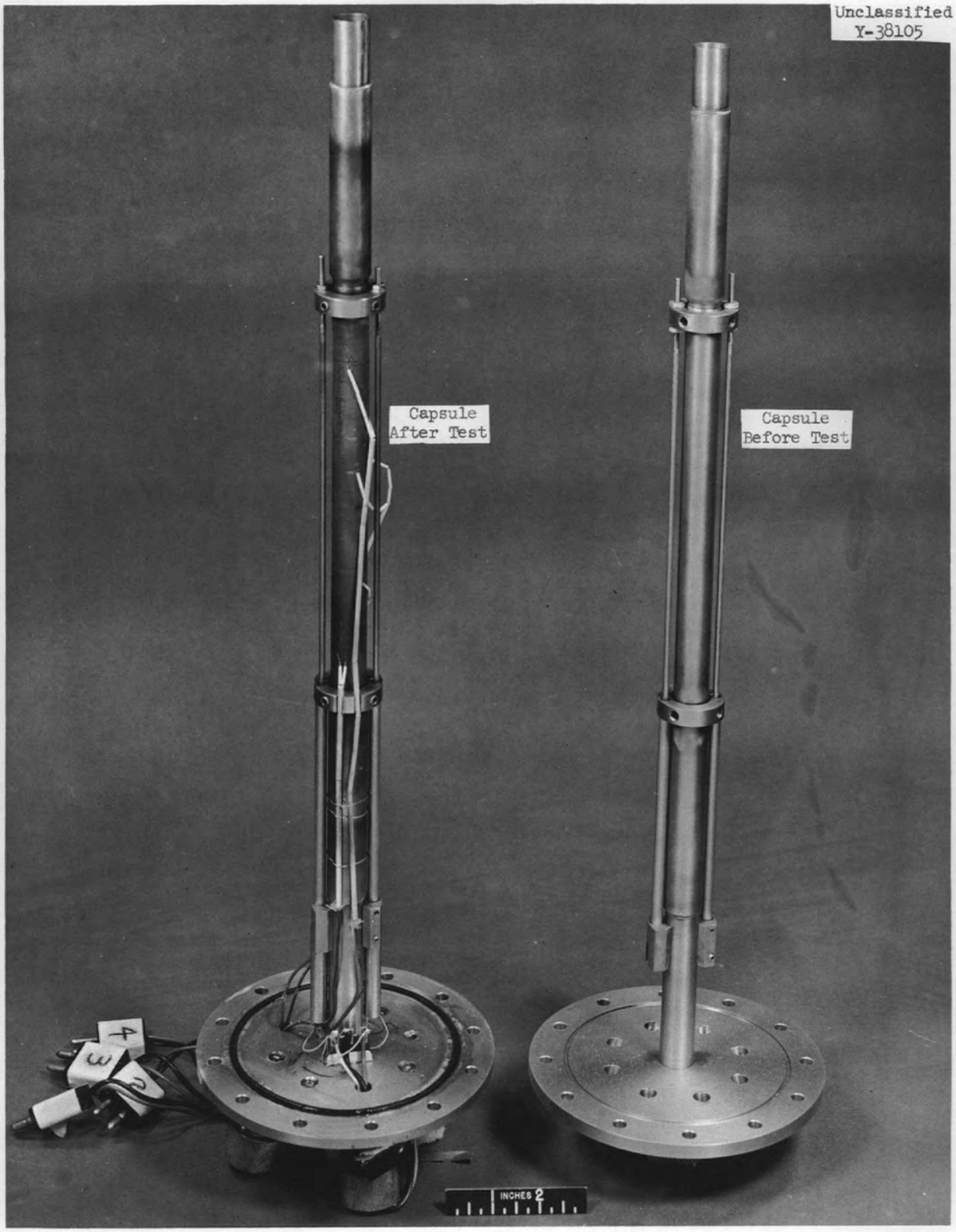

Fig. 17. Photograph of Simulated Element with Extensometer Before and After Test.

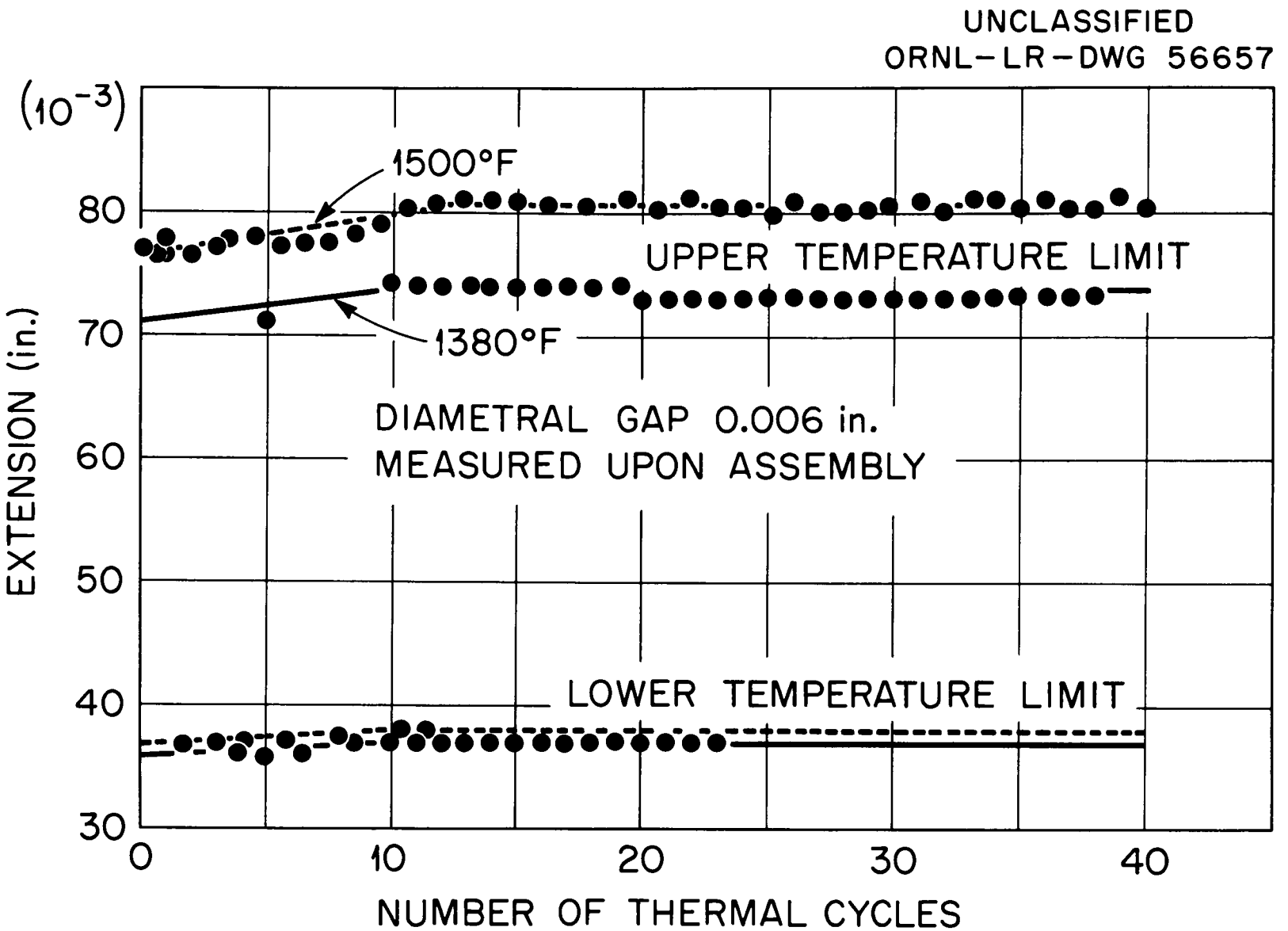

Fig. 18. Dimensional Behavior of Uncollapsed Fuel Capsule During Thermal Cycling.

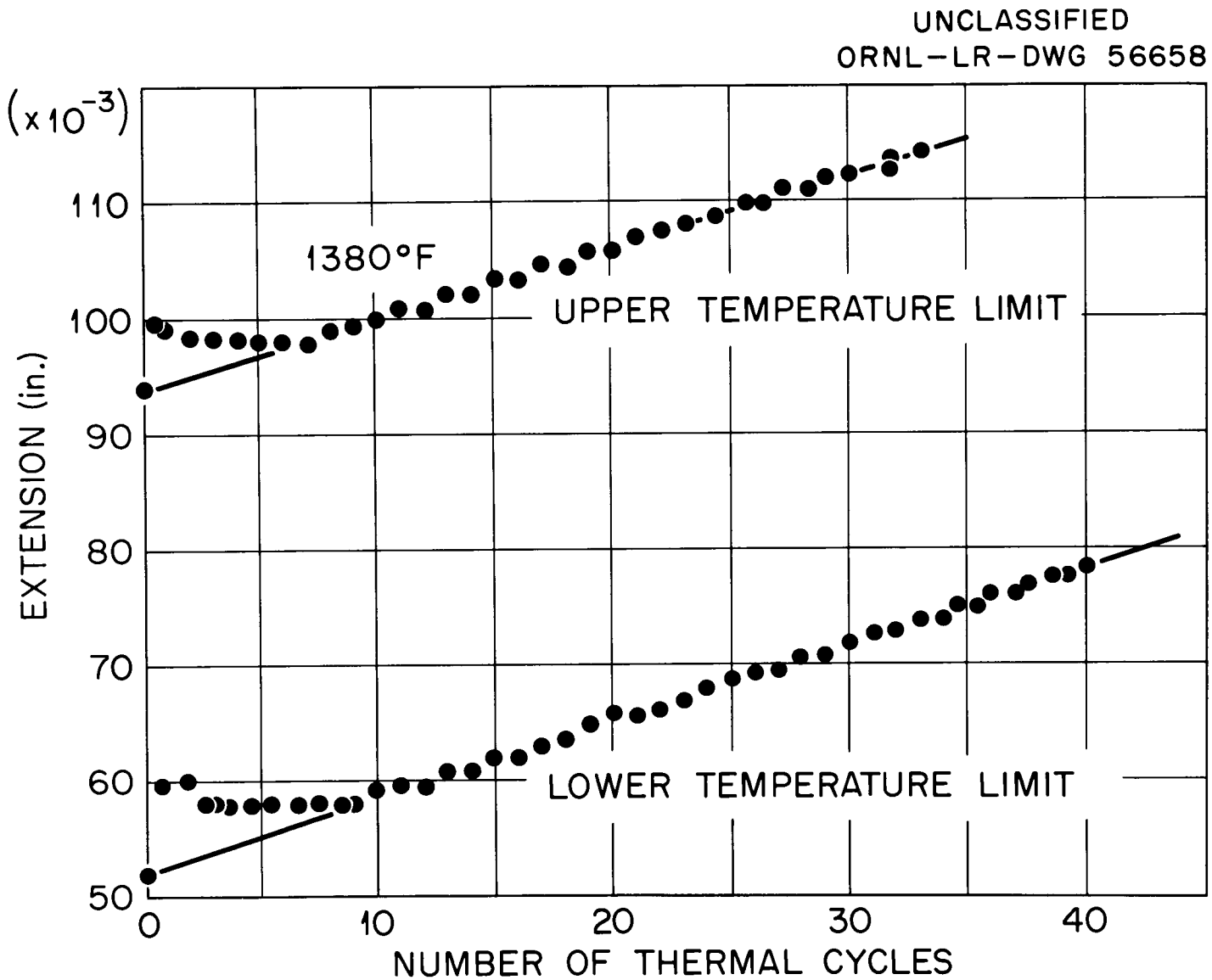

Fig. 19. Dimensional Behavior of Collapsed Fuel Capsule During Thermal Cycling.

prior to thermal cycling but was not subjected to external pressure, it may be concluded that another necessary condition is contact pressure between the cladding and the fuel. The permanent axial elongation per cycle as a function of the upper temperature limit is shown in Fig. 20. The family of curves shown in this figure illustrates that the strain varies as the lower temperature limit of the thermal cycling is varied. A cross plot, Fig. 21, shows a similar set of curves, each for different peak temperatures. The curves illustrate that both the upper and lower temperature limits of the cycles are important. The equation of the curves in Fig. 20 is of the form, $\epsilon_p/n = Ae^{-\Delta H/RT_1}$

where

ϵ_p/n = plastic strain per cycle,

ΔH = activation energy for high-temperature deformation,

R = gas constant,

T_1 = upper temperature limit of the thermal cycle, and

A = constant.

The equation therefore indicates the possibilities that a time-dependent, thermally activated deformation process results in the plastic strain. The constant, A, is a function of heating rate, cooling rate, hold time at temperature during cycling, and the temperature limit of the cycle.

For any cyclic operation in which the maximum cladding temperature during cycling is below 1325°F, the axial elongation during 50 cycles is not detectable. If the maximum temperature during cycling is above 1325°F, there is a lower temperature limit below which the capsule must be cycled before axial elongation of the cladding occurs.

The significance of other parameters, such as cooling and heating rate between the temperature limits of the cycle and the hold time at the upper temperature limit, has been investigated. The change in permanent elongation per cycle with heating and cooling rates is shown in Fig. 22. An increase of either heating or cooling rates increases the elongation rate. An increase in the heating rate results in a slightly larger axial elongation per cycle compared to an equivalent change in cooling rate. However, this difference is small and probably not significant. The magnitude of the axial elongation per cycle is

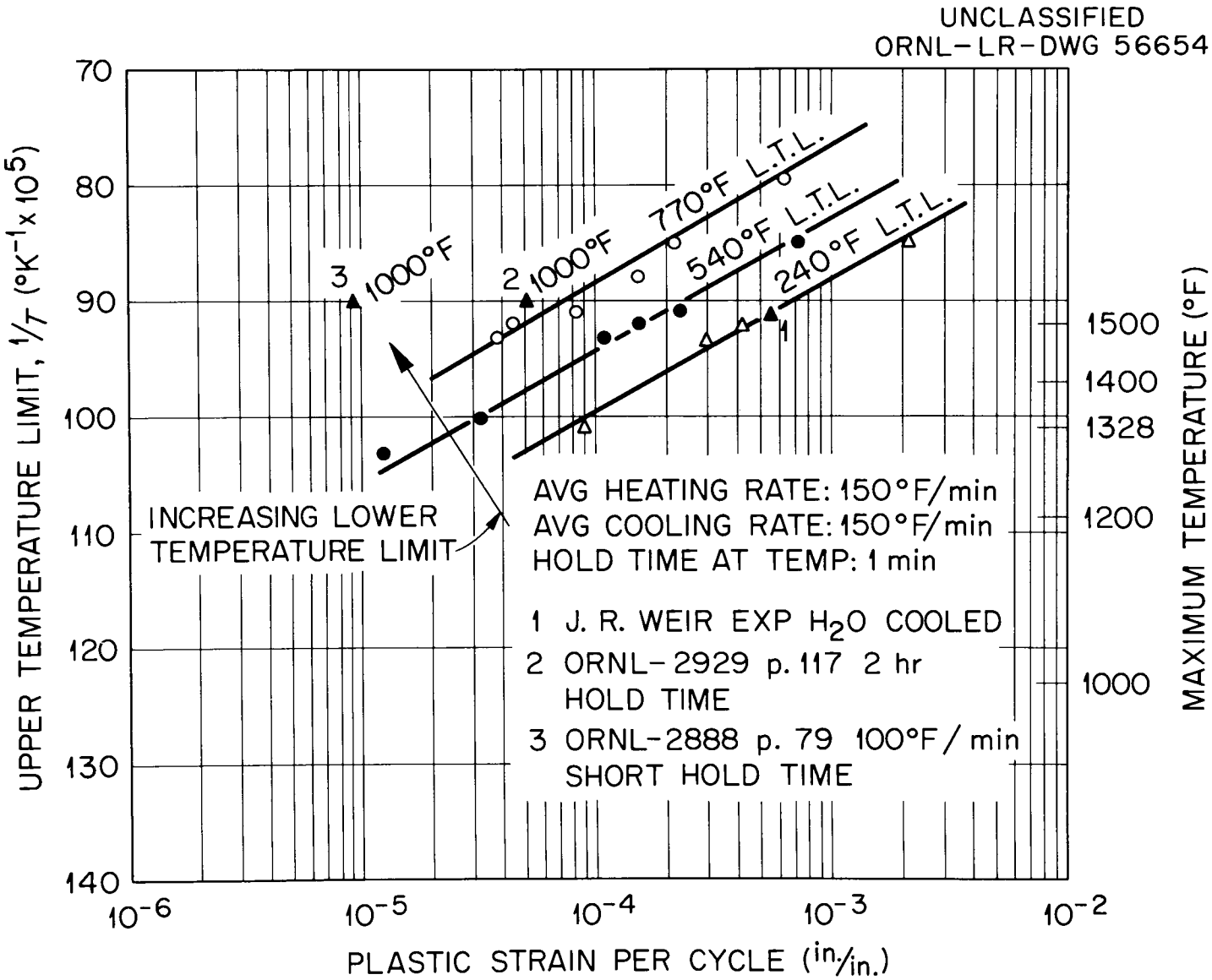

Fig. 20. Effect of Temperature Limits on Plastic Elongation of Thermal-Cycled Simulated EGCR Fuel Elements.

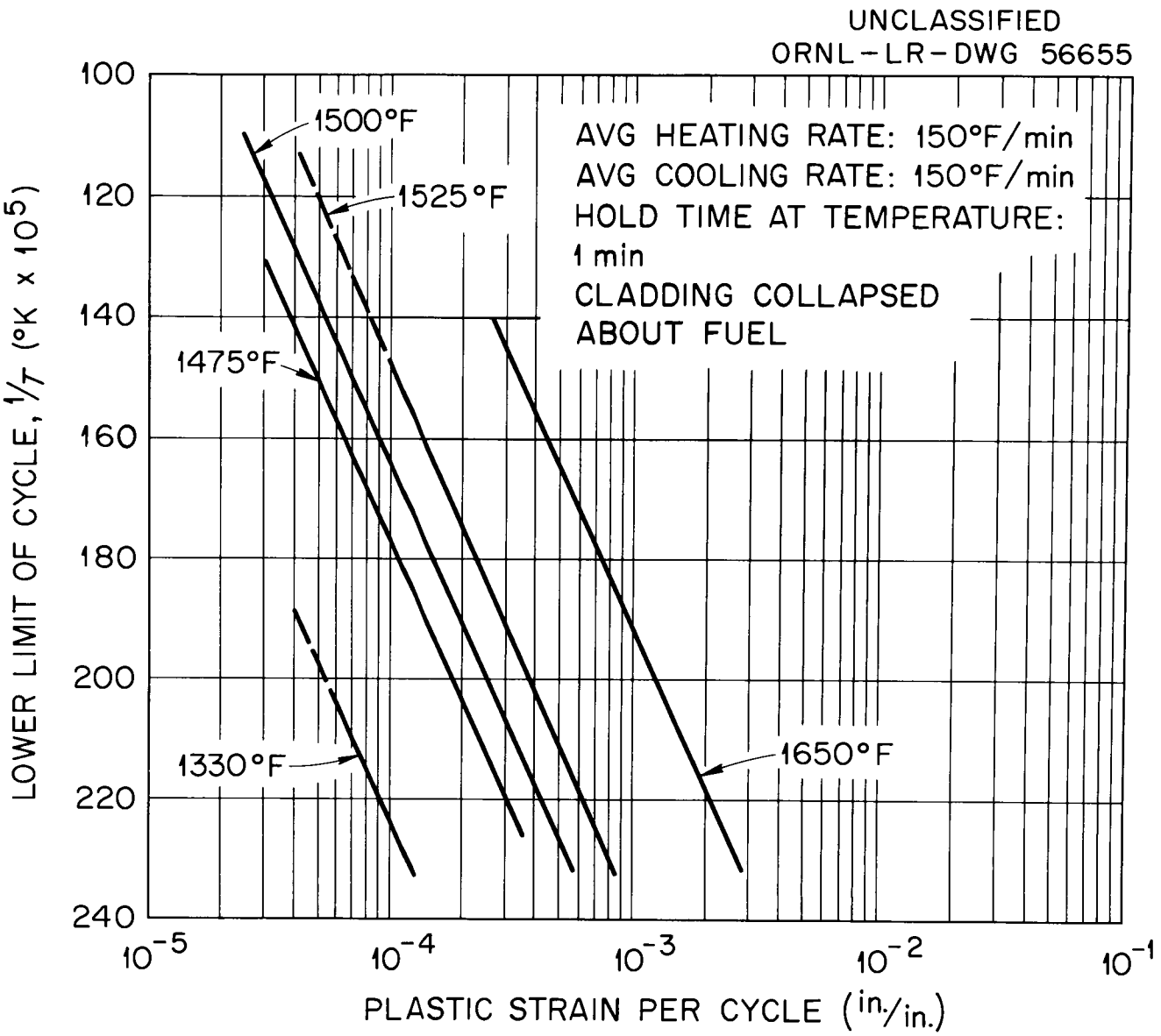

Fig. 21. Effect of Temperature Limits for Axial Elongation of Thermal-Cycled EGCR Fuel Capsule.

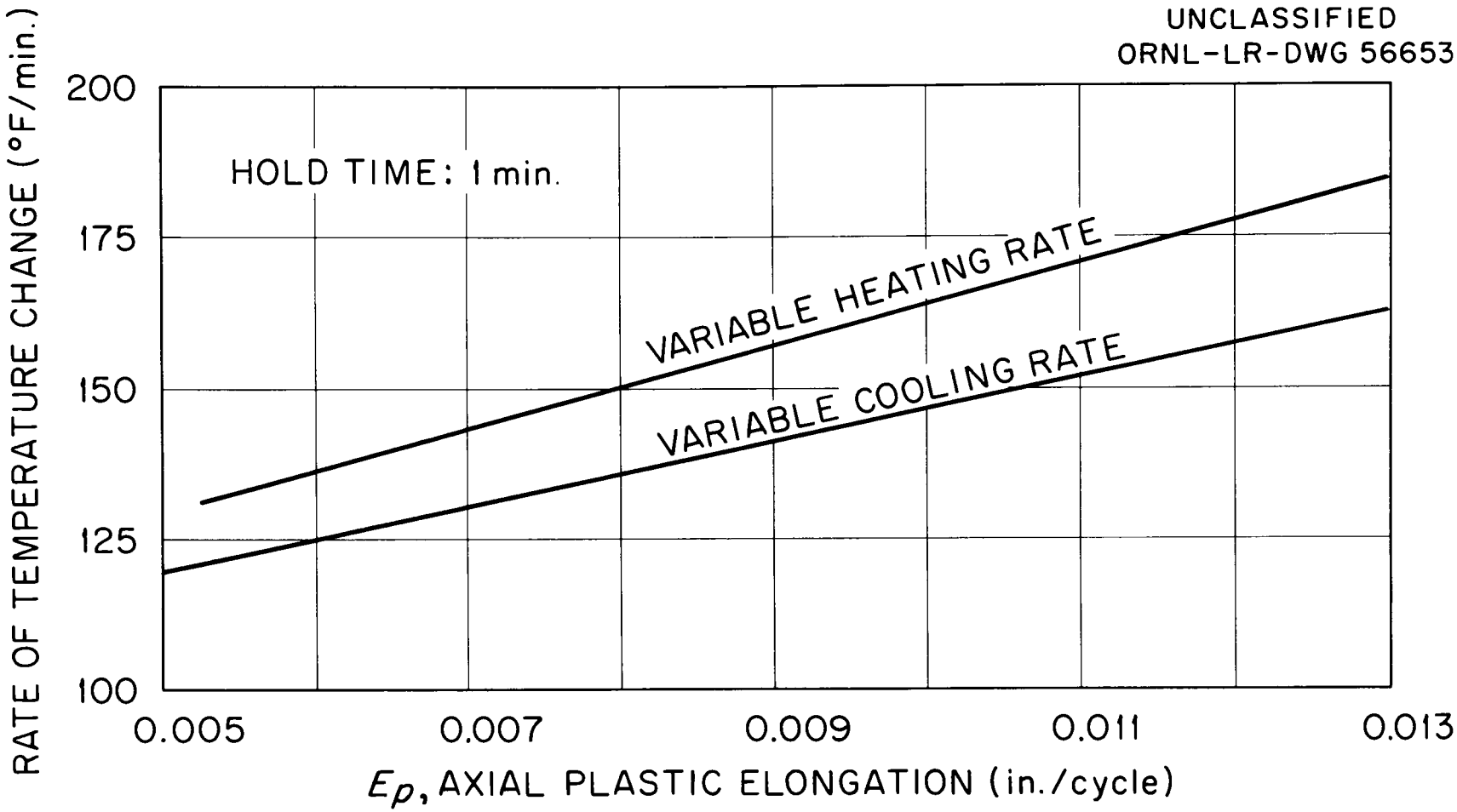

Fig. 22. Effect of Heating and Cooling Rate on Deformation Rate at 1500° F.

also dependent upon the hold time at the upper temperature limit as illustrated in Fig. 23. This curve is particularly interesting since it indicates that time-dependent deformation at the higher temperature is responsible for the axial growth of the cladding since zero plastic strain occurs at zero hold time. Hence, the relationships shown in Fig. 20 depend on the time at the upper temperature. As the hold time is increased from 1 to 20 min, the curves are shifted approx 1/2-log cycle to the right. Other investigators' data are shown in Fig. 20 referenced as notes 1 and 2 on the figure. Here again, an increase in hold time to 2 hr from a value less than 1 hr (the author did not report the actual hold time) has shifted the curve.

Physical Condition of Simulated Element After Test

As mentioned previously, circumferential ridges were formed during collapse of the capsule at positions which correspond to circumferential cracks in the pellets and at pellet interfaces. These ridges develop further during thermal cycling. This is shown rather clearly in Fig. 24a, a close-up view of a capsule thermal cycled with no diametral clearance. No localized thinning of the clad was found on examination of the sectioned simulated fuel capsules. The deformation which accompanies the ridge formation was generally uniformly distributed. During post-test examination of cycled capsules, it was found that the ridges are extremely difficult to measure and first appear as discolorations at the interface of the pellets within the capsule. Other investigators[13-16] have also found the ridge formation in irradiation experiments. A radiograph of very large ridges is shown in Fig. 24b. The occurrence of double ridges is shown in Fig. 24a.

---

[13] J. A. L. Robertson et al., "Irradiation Behavior of UO_2 Fuel Elements," Nuclear Metallurgy, Vol. 6, pp. 45–70, IMD Spec. Rep. Sev. No. 9, The Metallurgy Society of AIME, New York (1959).

[14] A. S. Bain, Behavior of Various Types of Zircaloy-2, Sheathed UO_2 Specimens Irradiated in the EEC Loop, FD-897 (1960).

[15] R. D. Paoge and J. A. L. Robertson, Atomic Energy of Canada Limited Progress Report, December 31, 1959, PR-CM-20, pp. 66–67.

[16] J. G. Morgan et al., GCR Quar. Prog. Rep. December 31, 1960, ORNL-3049, pp. 250–260.

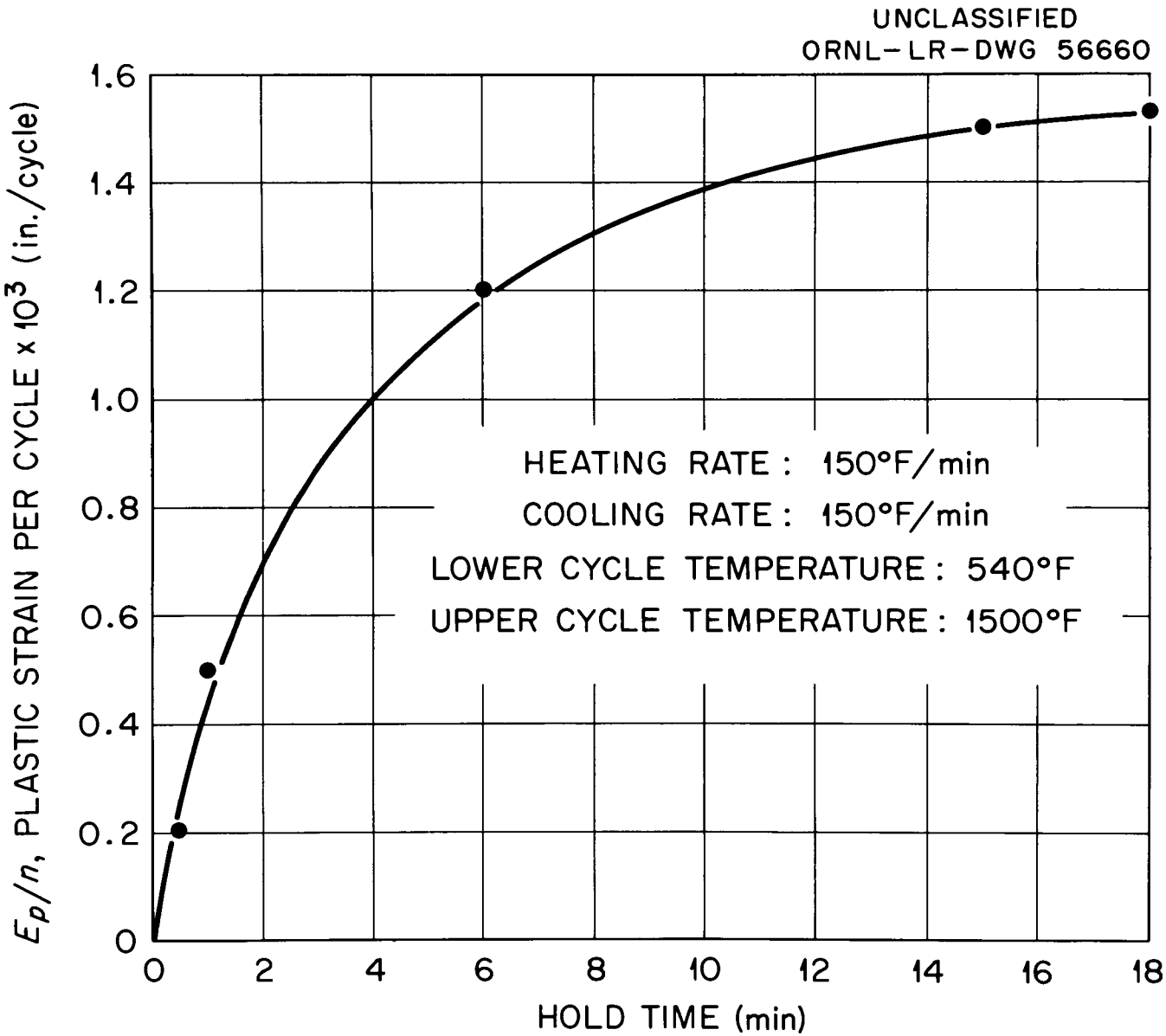

Fig. 23. Effect of Hold Time at Top of Cycle on Plastic Strain Per Cycle.

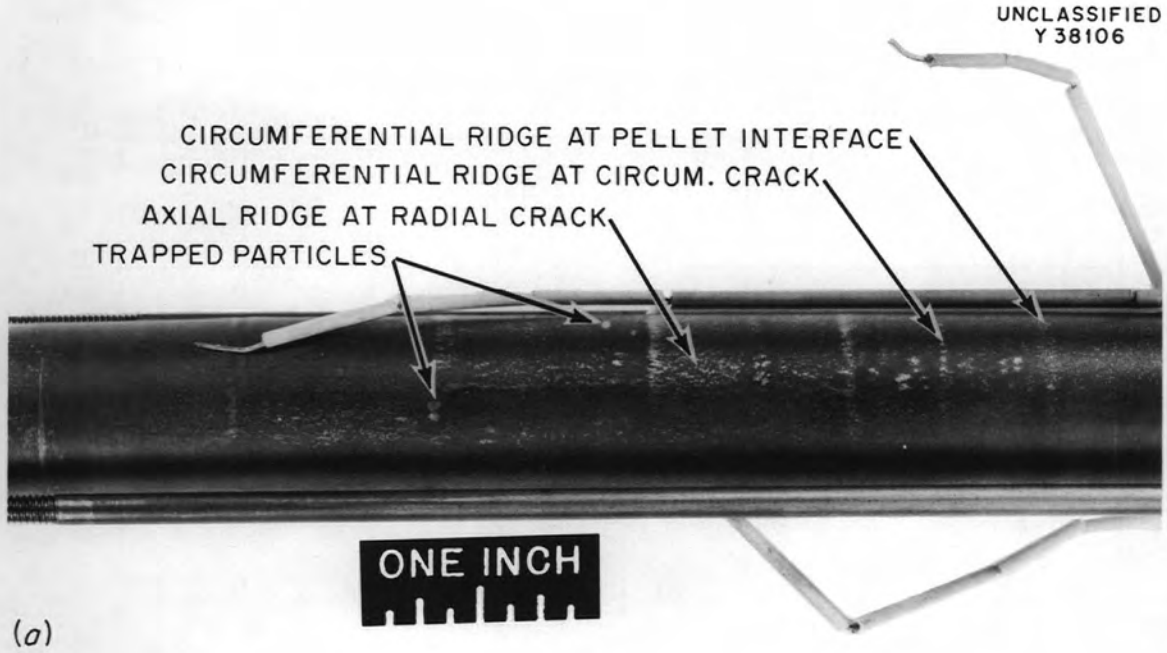

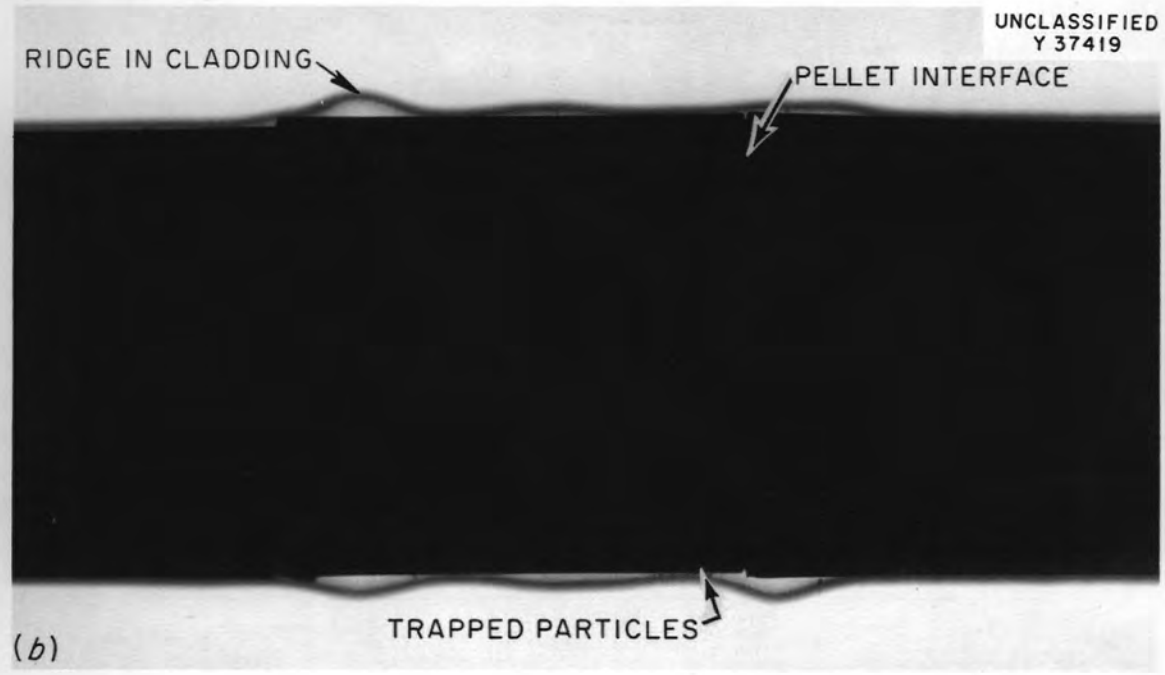

Fig. 24. (a) Photograph of Thermal-Cycled Capsule Showing Location of Circumferential and Axial Ridges.; (b) Photograph of Radiograph Indicating Maximum Ridge near Pellet to Pellet Interface. In the absence of external pressure, there is some relative movement between UO_2 and stainless steel during the cooling cycle. At temperature, the ridges were located at the pellet to pellet interface.

There is one axial ridge (Fig. 24a) which corresponds to the location of a radial crack in the UO_2 pellet. In this case due to thermal cycling before collapsing of the cladding, small UO_2 powder fines in the crack prevented its closing during collapse of the cladding. However, if the pellet is not subjected to thermal cycling before the cladding is collapsed, the radial crack in the UO_2 will close during collapse as shown in Fig. 25a. The microstructure of this area is shown in Fig. 25b to illustrate that the crack has closed. Thus, it appears that the formation of ridges in the fuel cladding will occur at any discontinuities in the UO_2 that form subsequent to collapse of the cladding if there is external pressure on the capsule. Figure 26 illustrates the result of contact pressure between fuel and cladding. The topography of the UO_2 surface, including a small crack, has been replicated on the inner surface of the cladding. Other experimenters have offered several suggestions, such as thermal stress, as the mechanism for ridge formation; however, no satisfactory mechanism has been presented. The axial load imposed on the cladding by the coolant stream may contribute, but is not entirely responsible for the circumferential ridges.

Particulates lodged in the radial gap shown in Fig. 27a and fragmenting of the fuel causing particle accumulation within the pellet-to-pellet interface shown in Fig. 27b of an uncollapsed element may cause difficulties if the element is in a reactor region where the cladding will collapse. It is interesting to note in Fig. 24a the existence of UO_2 particles that became lodged in the diametral gap between pellet and cladding during the thermal cycling before the collapsing operation. The imprint of each of the particles in the cladding clearly indicates their position. If fragmenting of the fuel similar to that shown in Fig. 27b were to occur, the larger gap between pellets could allow complete buckling of the cladding as was shown previously in Fig. 16. However, the behavior shown in Fig. 27b occurred in only one out of over 300 pellets used in the testing program and did not occur in fuel elements in which the cladding was collapsed prior to thermal cycling.

(a)

Unclassified
Y-35723

(b)

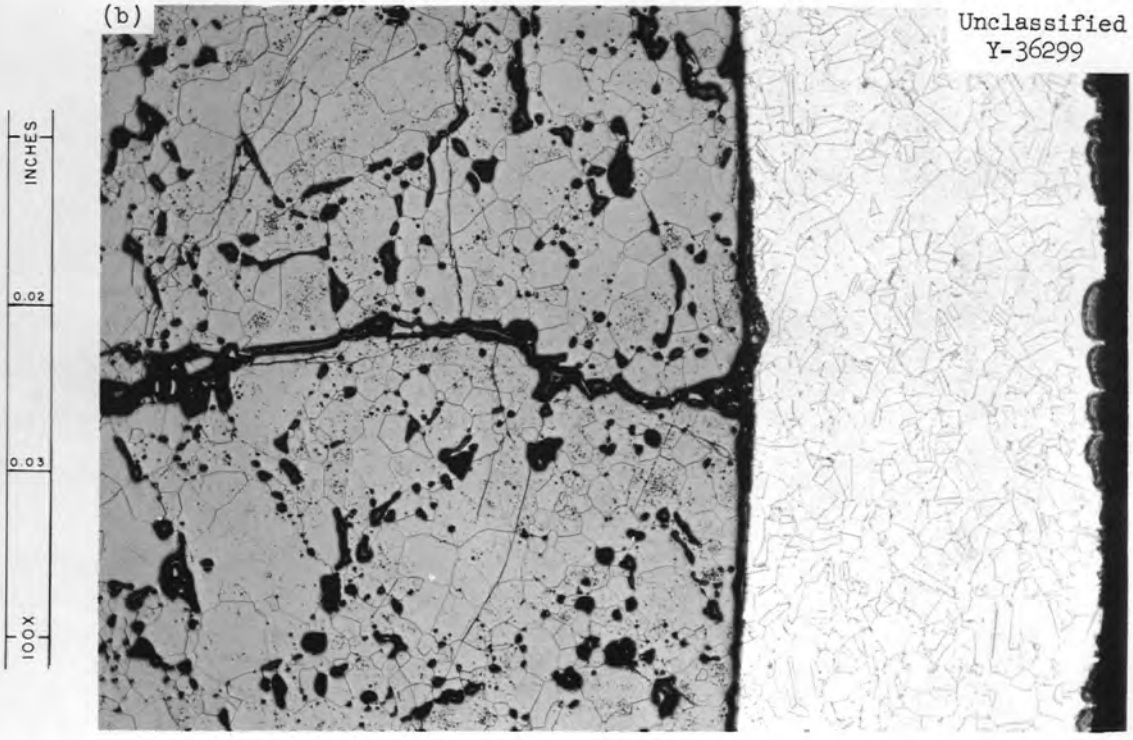

Unclassified
Y-36299

Fig. 25. (a) Photograph of Simulated Element Collapsed Before Thermal Cycling. Notice closure of radial crack. (b) Microstructure of Cross-Section Element Shown in Photograph 25a. Note deformed cladding due to trapped UO_2 Particles in the former radial gap.

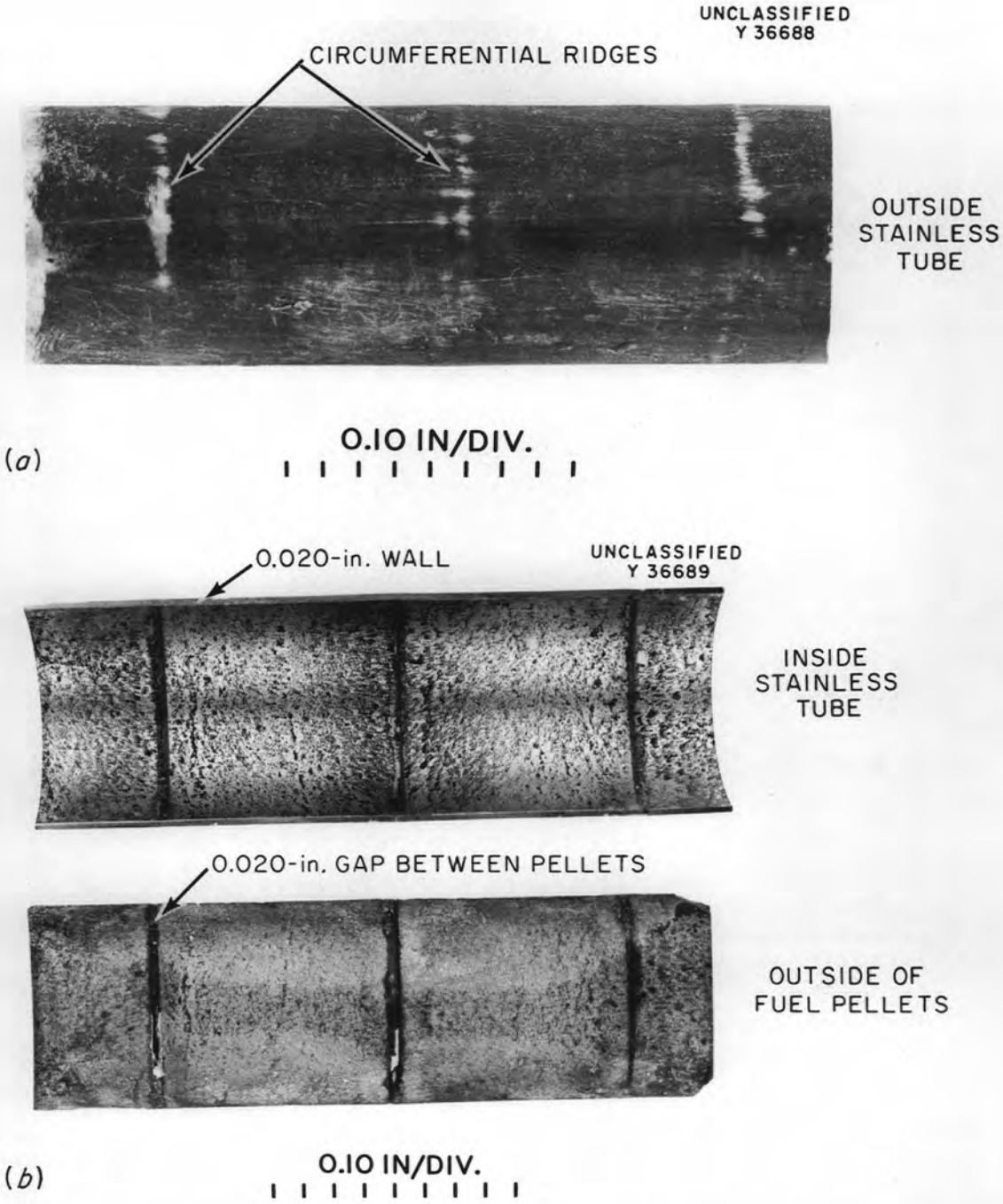

Fig. 26. (a) Photograph Showing Circumferential Ridges at Pellet Interface of Capsule Shown in Fig. 26b.; (b) Topography of UO_2 Surface, Including a Small Crack, has been Replicated on the Corner Surface of the Cladding which had been Collapsed about the Pellet.

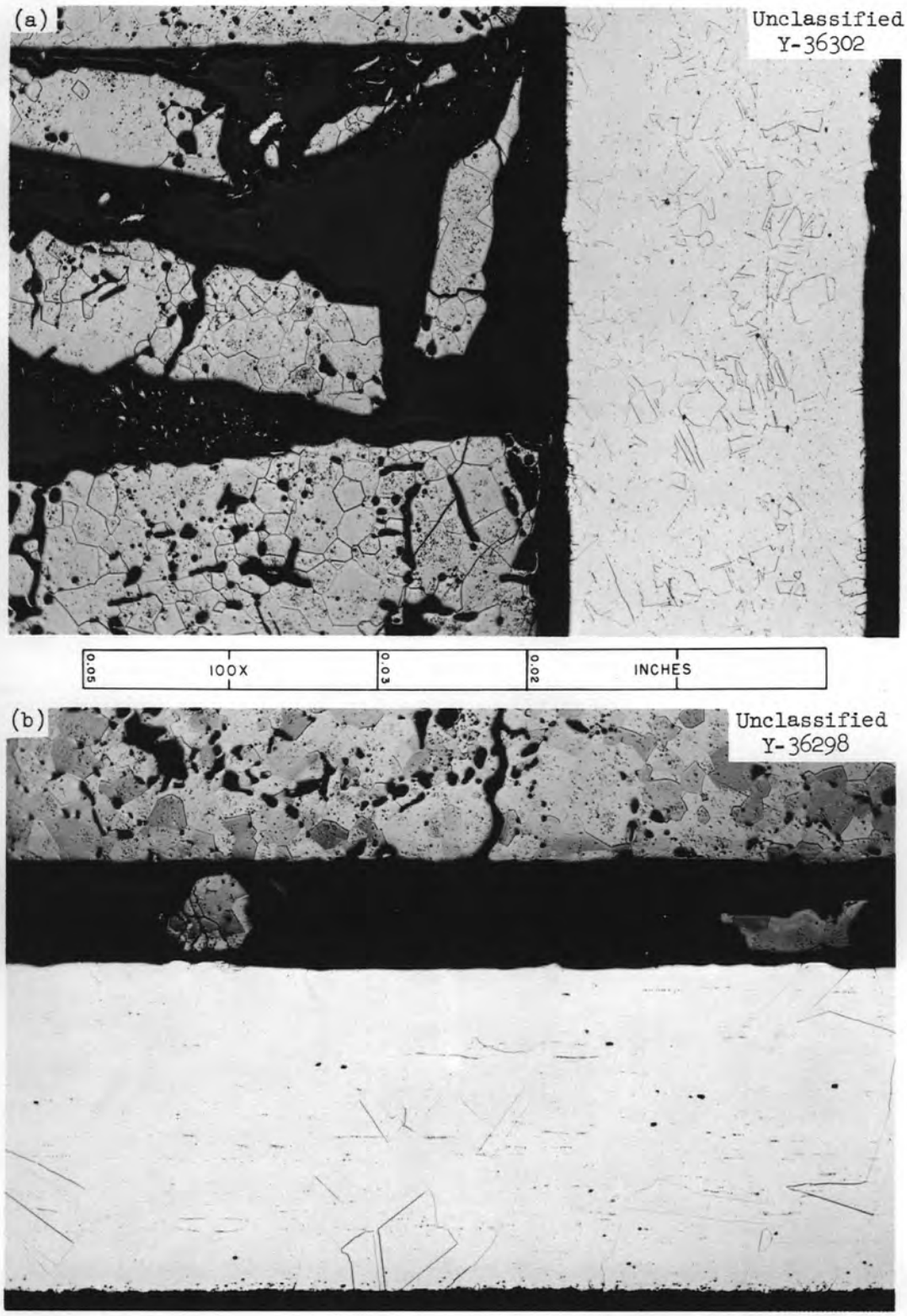

Fig. 27. (a) Photomicrograph Showing Fragmentation of UO_2 at Pellet-to-Pellet Interface of an Uncollapsed Capsule. (b) Photomicrograph Indicating Particulates in Radial Gap of Uncollapsed Capsule.

CONCLUSIONS

1. Both the radial and axial thermal expansion of either integral pellets or those fractured from thermal stress into smaller segments are a function of the maximum UO_2 temperature.

2. No structural changes[17] were found within the UO_2 pellets at short exposures to radial temperature gradients at maximum temperatures of 3400°F.

3. The total surface area of a given pellet is not a criterion on which the fracture strength of a pellet can be predicted or correlated within the accuracy of the surface area determination.

4. The fracture of UO_2 into fines as a result of thermal cycling was found to be insignificant. The fracture characteristics of the fuel were determined to be such that accumulation of fuel at the bottom of the vertical fuel element from cyclic operation will not occur. The effect of vibrations of the fuel element in the operating reactor on the fracture and formation of powder fines was not investigated.

5. The thermal-cycling behavior of a fuel element can be predicted from the expansion and fracture characteristics of the cladding and fuel if a radial gap exists at temperature between these components.

6. If the contact pressure between the fuel and clad is high, such as from collapse of the cladding about the fuel or high radial expansion of the fuel, plastic elongation of the element can result from thermal cycling. There is evidence that the deformation is thermally activated and time dependent. More refined and basic experiments on the element are needed before an accurate model for the growth of cladding can be constructed.

The program has experimentally demonstrated the dimensional behavior of a simulated fuel element exposed to thermal conditions predicted for the EGCR. Axial elongation of the capsule during thermal cycling has been measured and sufficient parameters investigated to be able to predict elongation of the capsule during actual reactor operation. The cladding has been severely deformed and the fuel thermal cycled without a single event which could be defined as an element failure.

---

[17] V. B. Lawson and J. R. MacEwan, Structural Changes Within UO_2 Pellets Subjected to a Temperature Gradient, CRFD-915 (March, 1960).

ACKNOWLEDGMENTS

The authors are grateful for the support and help of all the Mechanical Properties Group, particularly K. Boling who performed the tests, and the assistance of K. K. Klindt of Inspection Engineering Department for radiographic service work.

DISTRIBUTION

1. Biology Library
2. Health Physics Library
3. Metallurgy Library
4–5. Central Research Library
6. Reactor Division Library
7. ORNL – Y-12 Technical Library Document Reference Section
8–27. Laboratory Records Department
28. Laboratory Records, ORNL R. C.
29. G. M. Adamson, Jr.
30. D. S. Billington
31. A. L. Boch
32. E. G. Bohlmann
33. B. S. Borie
34. R. B. Briggs
35. C. E. Center
36. R. A. Charpie
37. R. S. Cockreham
38. E. Cohn
39. J. H. Coobs
40. F. L. Culler
41. J. E. Cunningham
42. D. A. Douglas, Jr.
43. J. H Frye, Jr.
44. A. Goldman
45. W. R. Grimes
46. W. O. Harms
47. C. S. Harrill
48–52. M. R. Hill
53. E. E. Hoffman
54. A. Hollaender
55. A. S. Householder
56. R. G. Jordan (Y-12)
57. W. H. Jordan
58. C. P. Keim
59. M. T. Kelley
60. J. A. Lane
61. R. S. Livingston
62. H. G. MacPherson
63. W. D. Manly
64–73. W. R. Martin
74. C. J. McHargue
75. A. J. Miller
76. E. C. Miller
77. J. G. Morgan
78. K. Z. Morgan
79. J. P. Murray (K-25)
80. M. L. Nelson
81. P. Patriarca
82. D. Phillips
83. P. M. Reyling
84. G. Samuels
85. H. W. Savage
86. J. L. Scott
87. H. E. Seagren
88. E. D. Shipley
89. M. J. Skinner
90. C. O. Smith
91. A. H. Snell
92. J. A. Swartout
93. E. H. Taylor
94. W. C. Thurber
95. D. Trauger
96. A. M. Weinberg
97. J. R. Weir
98. E. Wick
99. J. C. Wilson
100. C. E. Winters
101. A. A. Burr (consultant)
102. J. H. Koenig (consultant)
103. C. S. Smith (consultant)
104. R. Smoluchowski (consultant)

EXTERNAL DISTRIBUTION

105. D. E. Baker, GE Hanford
106–107. D. Cope, ORO
108. Bruce Dunnington, Battelle Memorial Institute
109. Ersel Evans, GE Hanford
110. Ronald Fillnow, Westinghouse Electric, Bettis Atomic Power Division, Pittsburgh

EXTERNAL DISTRIBUTION, continued

111. Art Foche, GE ANPD, Cincinnati, Ohio
112. J. L. Gregg, Cornell Univ.
113. E. E. Hayes, du Pont Company, Wilmington, Delaware
114. B. R. Hayward, Atomics International, Canoga Park, California
115. J. H. Kettel, Argonne National Laboratory, Argonne, Illinois
116. K. Kobelt, Parma Research Center Library, Parma, Ohio
117. George Last, GE Hanford
118. D. Lesser, Atomic Power Development Associates, Inc., Detroit
119. E. E. Stansbury, Univ. of Tenn.
120. Donald K. Stevens, AEC, Washington
121. J. Simmons, AEC, Washington
122. B. Weidenbaum, Vallecitos Atomic Laboratory, Pleasanton, California
123. Walter Wallace, General Atomics, San Diego, California
124-625. Given Distribution as shown in TID-4500 (16th ed.) under Metals, Ceramics, and Materials Category.
626. Division of Research and Development, AEC, ORO